Chapter 2
Carbon-Concentrating Mechanism

2.1 Introduction

None of the element on earth is more essential to life than carbon. Every living molecular machine is constructed across a middle staging of organic carbon. Unfortunately, carbon in the planet is locked in extremely oxidized structures, such as carbonate minerals (calcite, aragonite, etc.) and CO_2 gas (Walker 1985). In order to be functional, these oxidized structures ought to be unlocked and transformed into more organic forms, rich in C=C bonds and decorated with hydrogen atoms. With the help of light energy of sun, photosynthetic organisms perform this central task of carbon transformation in nature through the process called "photosynthesis." Among photosynthetic organisms, photosynthetic microorganisms (such as cyanobacteria and microalgae) play a significant role in the formation of organic biomass and oxygenic environment on Earth. They generate nearly half of the primary products of biosphere by contributing a large portion of carbon capture (Falkowski and Raven 1997). Majority of photosynthetic microorganisms undertake photosynthesis in an aquatic environment of ocean where they face a number of unique restraints regarding the efficient operation of carbon fixation through photosynthesis. In response to ancient changes in atmospheric CO_2 and O_2 levels, the photosynthetic microorganisms evolved a unique environmental adaptation, known as a CO_2-concentrating mechanism (CCM) (Badger and Price 2003), which has a significant positive effect on photosynthetic performance. In recent years, a deeper understanding of the mechanisms and genes underlying the operation of CCM has been increased rapidly.

2.2 Photosynthesis: Basis of Life on Planet

Photosynthesis (Greek: phos "light" and syntithenai "put together") is a central route in the global carbon cycle which serves as single prevalent flux of organic carbon in biosphere (Kirk 1994). It is a complex physico–chemical process occurs in a diverse group of organisms by which light energy from sunlight is absorbed

S.K. Singh et al., *Photosynthetic Microorganisms*, SpringerBriefs in Materials,
DOI 10.1007/978-3-319-09123-5_2

by pigments and converted into chemical energy in the form of organic carbohydrates using carbon dioxide (CO_2) and water (See Eq. 2.1).

$$6CO_2 + 12H_2O + \text{Nutrients} + \text{Sun Light} \rightarrow C_6H_{12}O_6 + 6O_2 + 6H_2O \quad (2.1)$$

The photosynthesis process occurs widely in green pigments containing plants, algae, photosynthetic bacteria, and aerobic anoxygenic phototrophic bacteria which results in the release of molecular oxygen and the removal of CO_2 from the atmosphere that is used to synthesize carbohydrates (Shiba et al. 1979; Yurkov and Beatty 1998).

2.2.1 Basic Mechanism of Photosynthesis

The photosynthesis process encompasses two universal phases (Fig. 2.1).

In the first phase, "light-dependent reactions" involve light absorption, water splitting for electrons and protons source, generation of energy currencies such as NADPH and ATP and oxygen release as a by-product (Kirk 1994). The high-energy chemical intermediates, ATP and NADPH, further utilized as an energy source for the sequence of second phase "light-independent reactions" to fix CO_2 and reduce C_i in triose phosphates (carbohydrate precursors). Over all view of the whole photosynthesis process is shown in Fig. 2.2.

2.2.1.1 Light-Dependent Reactions

The light-dependent reactions are a sequence of chemical reactions occurs at the concentrated stacks of thylakoid called grana. It required the straight energy from

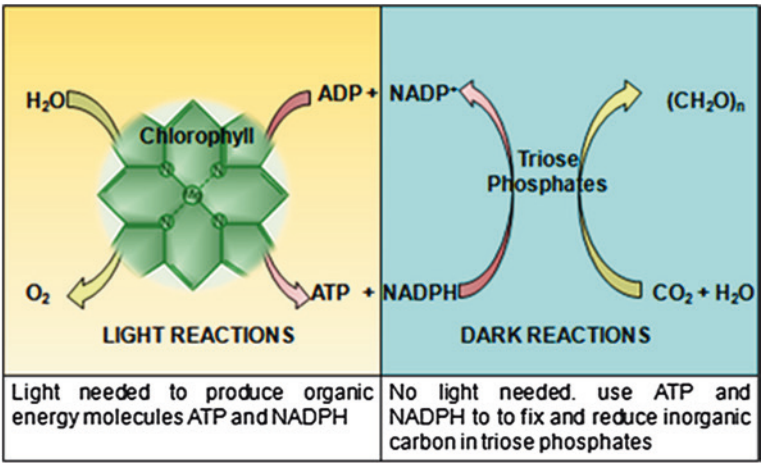

Fig. 2.1 Universal phases of photosynthesis process

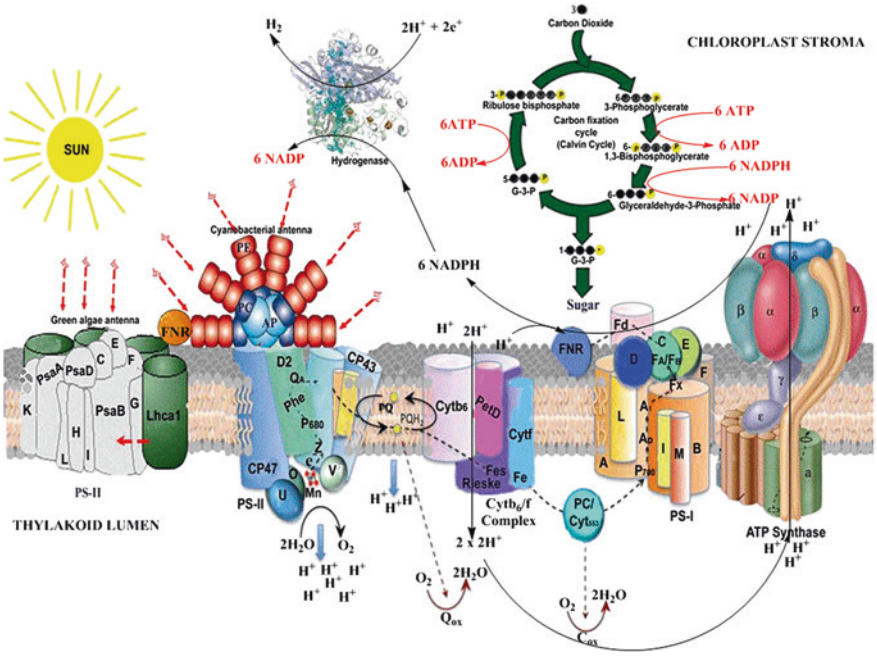

Fig. 2.2 Detailed view of light and dark reaction of photosynthesis

sunlight to make energy-carrier molecules (ATP and NADPH), which further used later in the light-independent reactions. The energy to drive light-dependent reactions comes from two photosystems: Photosystem II (PSII/P_{680}) and Photosystem I (PSI/P_{700}) (Barber 2003). The core of a photosystem is made of three molecules: a chlorophyll molecule, an electron acceptor (e.g., pheophytin), and an electron donor (e.g., water) (Van Gorkom 1985). All photosynthetic organisms have chlorophyll a and accessory pigments which include chlorophyll b (also c, d, and e in algae and protistans), xanthophylls, phycocyanin and phycoerythrin (cyanobacteria), and carotenoids (such as β-carotene) (Dufossae et al. 2005). Accessory pigments help to absorb light energy that chlorophyll a does not absorb. Initially, at PSII, light energy is absorbed by a chlorophyll molecule, an electron gains energy and is "excited" (photoexcitation). The excited electron is further transferred to a primary electron acceptor (Scholes and Fleming 2005), leaving a positively charged chlorophyll ion (photoionization). The positively charged chlorophyll ion then takes a pair of electrons from a splitting of two molecules of water (oxidized, i.e., loses electrons) into one molecule of molecular oxygen (see Eq. 2.2).

$$2H_2O \rightarrow 4H^+ + O_2 + 4e^- \text{(photolysis)} \tag{2.2}$$

The four electrons removed from the water molecules are transferred by an electron transport chain to ultimately reduce two molecule of nicotinamide adenine

dinucleotide phosphate ($NADP^+$ to NADPH) (see Eq. 2.3). During the electron transport process, a proton gradient is generated across the thylakoid membrane. This proton motive force is then used to drive the synthesis of ATP (photophosphorylation) (see Eq. 2.4). This process requires PSI, PSII, cytochrome b_6f, ferredoxin-$NADP^+$ reductase, and chloroplast ATP synthase.

$$\text{nADP} + \text{nP}_\text{i} + \text{photons} \rightarrow \text{nATP} \tag{2.3}$$

$$\text{NADP}^+ + 2\text{e}^- + 2\text{H}^+ \rightarrow \text{NADPH} + \text{H}^+ \tag{2.4}$$

The final stage of the light reactions is catalyzed by PSI. This protein has two main subunits forming its core antenna system, *psa*A and *psa*B. A special pair of chlorophyll a molecules, denoted as P_{700}, lies at the center of the structure, and absorbs light maximally at 700 nm wavelength (Green and Parson 2003). Upon excitation, P_{700} transfers an electron through chlorophyll and a bound quinone (Q_A) to ferredoxin (F_d) (electron acceptor), a water soluble mobile electron carrier located in the stroma (Gilbert et al. 2012). The electron transfer constructs a positive charge on the P_{700}, which is neutralized by the transfer of an electron from a reduced plastocyanin (electron donor). The electron transport chain from PSII to cytochrome b_6f to PSI is known as Z-scheme as redox diagram looks like letter Z.

2.2.1.2 Light-Independent Reactions

In the light-independent process (the Dark reaction), CO_2 from the atmosphere or water (for aquatic photosynthetic organisms) is captured and subsequently transformed by the addition of hydrogen to reduced carbon form such as carbohydrates (Schuster et al. 1984). The energy for this process comes from the first phase of the photosynthetic process. The incorporation of CO_2 into organic compounds is known as carbon fixation which we will discuss in more detail later in the chapter.

Although photosynthesis process occurs in tiny micron-sized cells or organelles, it has a profound impact on the world's atmosphere and climate (Whitmarsh 1999). Each year, this CO_2 anabolic process helps in the transformation of approximately 100 billion tons of atmospheric carbon, which corresponds to almost 15 % of carbon in atmosphere (Raines 2011). Only within the last couple of decades, recent resurgence in basic and applied research on photosynthesis has been driven in part by recognition of novel strategies for compartmentalizing and enhancing the rates of photosynthetic carbon fixation reactions in a species-independent manner. Among all photosynthetic organisms, aquatic photosynthetic microorganisms face several challenges in acquiring CO_2 from the environment. Knowledge of CO_2 fixation in aquatic photosynthetic organisms is vital to understand the ecology between aquatic photosynthetic organisms and earth's atmosphere, for maintaining the equilibrium of organic carbon in biosphere.

2.3 Carbon-Concentrating Mechanism (CCM): A Potential Tool to Sequester Carbon

Carbon-concentrating mechanism (CCM) is a remarkable adaptation, evolved to maximize photosynthetic efficiency of many photosynthetic organisms in low-CO_2 (L-CO_2) environment. Since their role was first discovered (Badger et al. 1980), the mechanisms assisting the endurance of photosynthetic cells in L-CO_2 conditions have continued to be intensively studied. Concerns of sustainability, future food, and energy requirements are also motivating the researchers to elucidate the CCM machinery. Although in the last decade, significant progresses have been made to understand the exact CCM machinery of photosynthetic microorganism (Badger and Price 2003; Tabita et al. 2008; Whitney et al. 2011; Warlick 2013). However, many functional factors of CCMs are still unidentified or uncharacterized. The CCM is often an inducible process, and hence, the sensing of the lowering of CO_2 both intra- and extracellularly is needed to drive the structural and biochemical changes that accompany CCM induction. The signals that activate CCM have not been totally explored. More than one molecular inducer might exist to convey about the activation of genes and proteins central to the CCM process and the L-CO_2 adaptation of photosynthetic microorganism cells. The majority of evaluated aquatic CCMs are related to cyanobacteria and microalgae species (Raven et al. 2008; Reinfelder 2011, Ducat and Silver 2012; Barsanti and Gualtieri 2014).

2.3.1 Why Photosynthetic Microorganisms Need CCM?

Quite a number of photosynthetic microorganisms face the following key challenges of photosynthesis in aquatic environment.

2.3.1.1 Rate of Diffusion of CO_2

Since the energy transformations occurring in metabolism of living organisms are chiefly brought about by chemical changes in carbon-based biomolecules, the absorption and assimilation of CO_2 cannot be considered apart. In aqueous environment, the rate of diffusion of CO_2 is 10,000 times slower than the diffusion of CO_2 in air (Moroney and Ynalvez 2007). So that, there is relative equilibrium of CO_2 between air and water, which can result in carbon stress by causing a depletion of inorganic carbon (C_i) species including, CO_2, HCO_3^-, and CO_3^{2-} in water during active photosynthesis conditions. Furthermore, the photosynthetic microorganism growth environments are also subjected to fluctuations in C_i concentrations (CO_2 and HCO_3^-) due to pH (see Eq. 2.5)

$$CO_2 + H_2O \underset{\text{Slow}}{\overset{pKa_1=6.35}{\longleftrightarrow}} HCO_3^- + H^+ \underset{\text{Fast}}{\overset{pKa_2=6.35}{\longleftrightarrow}} CO_3^{2-} + H^+ \tag{2.5}$$

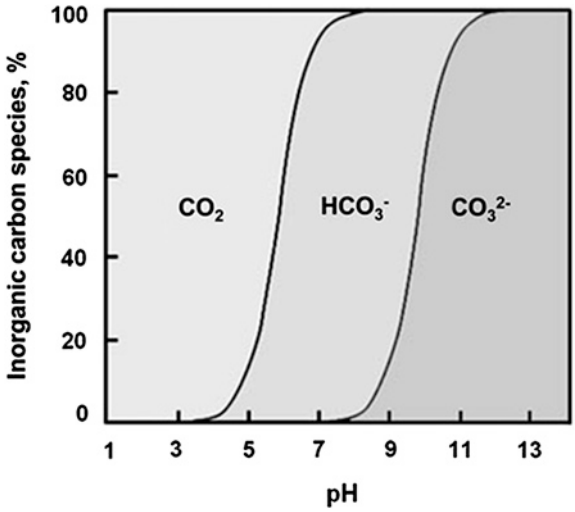

Fig. 2.3 Transformation of inorganic carbon forms at different pH

At the normal or slightly alkaline pH, water is typically low (approximately 10 μM) in CO_2 concentration (Lapointe et al. 2008), and causes the prevalence of less diffusible C_i form, HCO_3^-. It all affects the photosynthesis process that becomes carbon limited due to depletion of CO_2 from their instantaneous vicinity. The capability to scavenge CO_2 as rapidly as it becomes accessible is extremely advantageous to aquatic photosynthetic microorganisms. Figure 2.3 depicts aspects of this supply problem.

2.3.1.2 Limitations of RuBisCO

Despite its essential part in carbon fixation ability of photosynthetic organisms, ribulose bisphosphate carboxylase–oxygenase (RuBisCO) is, however, an unusual slow enzyme with a low affinity for CO_2. The catalytic ineffectiveness of RuBisCO originates not only from its low turnover rates but also exacerbated by O_2, being a competitive substrate of CO_2 in two competing reactions, carboxylation and oxygenation (Portis and Parry 2007). At atmospheric concentrations of CO_2, RuBisCO can only function at about one fourth of its catalytic capacity (Moroney and Ynalvez 2007). The existence of oxygen as a prevalent competitive substrate of CO_2 causes the redirection of fixed carbon into the photorespiratory cycle directing to the loss of at least 30 % of carbon fixed by RuBisCO (Raines 2011). As a result, all different CCMs form of aqueous photosynthetic organisms have evolved adaptations with a common aim of elevating CO_2 around RuBisCO to alter the CO_2/O_2 ratios at the active site in favor of the carboxylase reaction. In this manner, CCMs minimize the costly investment of metabolic energy and carbon in the photorespiration (Raven et al. 2008).

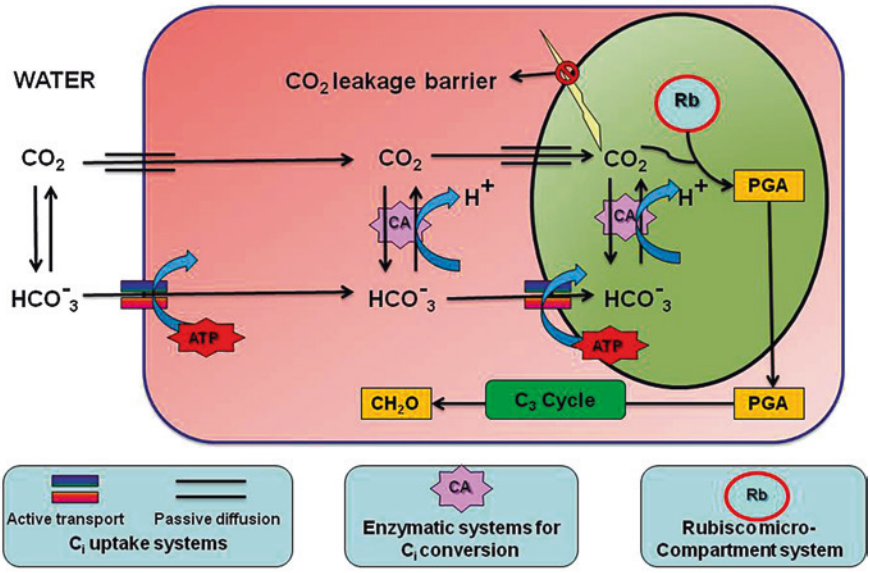

Fig. 2.4 Elements of photosynthetic microorganism CCMs

2.3.2 Functional Elements of Photosynthetic Microorganism CCMs

Even though, the complexity of cellular components and abilities of CCMs varies in different organisms, they have three major operational systems in common that allow them to achieve an effective use of CO_2. These are depicted in Fig. 2.4 and include the following.

2.3.2.1 Inorganic Carbon (C_i) Uptake Systems

The C_i uptake system*s* play a central role to achieve a satisfactory rate of CO_2 fixation into the cells of photosynthetic microorganisms under limiting carbon conditions. Photosynthetic microorganisms can use both form of C_i, ionic bicarbonate ions, and neutral CO_2 molecules. The maneuver of the C_i uptake systems enhances cytosolic concentrations of C_i to thousand times greater than extracellular concentrations (Daley et al. 2012). The C_i uptake system in photosynthetic microorganisms comprised of different HCO_3^- transporters and CO_2 uptake systems. Uptake machinery assists in the transfer, accumulation, and utilization of C_i as well as also prevents the diffusive leakage of CO_2 from actively photosynthesizing cells (Mukherjee 2013). The mechanism of C_i uptake is different in prokaryotes and eukaryotes photosynthetic microorganisms. Neutral molecules of CO_2

may passively enter a cell by direct diffusion while negatively charged HCO_3^- requires energy-driven transporters. These transporters may contrast in their affinity and diffusion rate of C_i. Most prokaryotic cyanobacteria possess energy-driven active systems for C_i uptake, however, eukaryotic microalgae relies on the pH gradient setup across the chloroplast thylakoid membrane in the light. In addition, the electrochemical gradient may also be consumed for the symport transportation in eukaryotic microalgae (Price 2011).

2.3.2.2 Enzymatic System for C_i Conversion

Neutral molecules of CO_2 may diffuse passively inside a cell, due to their high solubility in membrane lipids (Mukherjee 2013). This could be very nice in terms of energy saving; however, CO_2 may simultaneously, and with same efficiency, diffuse back out of the cells. This challenge is solved by carbonic anhydrase (CA)-based enzymatic system which catalyzes the rapid conversion of transferred CO_2 into HCO_3^- and vice versa, inside the cell (Tsuzuki and Miyachi 1989). Since, negatively charged HCO_3^- is almost thousand times less permeable to the lipid membranes than neutral CO_2 species (Price 2011). Thus, particularly at 7.8–8.2 cytoplasmic pH, CO_2 could be the ideal form of C_i for assimilation in cell while HCO_3^- form helps in preventing the outward leakage of C_i back into the medium. Various active CAs are localized at various sites in the cell predominantly close to the vicinity of RuBisCO where the level of CO_2 essentially to be elevated for proper CCM working (Mukherjee 2013).

Carbonic Anhydrases

The CAs (carbonate hydrolyase, E.C. 4.2.1.1) are ubiquitous metalloenzymes (mainly Zn) that catalyzes the quick reversible hydration reaction of CO_2 to HCO_3^- and protons (H^+) or vice versa. This "reverse" reaction gives CA its name, because it removes a water molecule from carbonic acid (see Eq. 2.6).

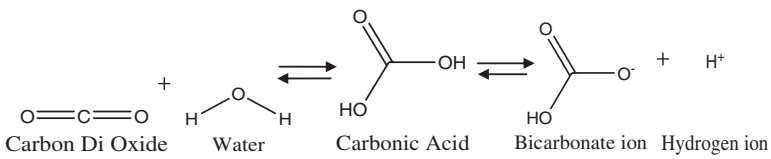

(2.6)

Due to the vital biocatalyst role of CAs, nature has advanced its catalytic ability as one of the fastest of all enzymes, to hydrate carbon dioxide and dehydrate bicarbonate a number of times (turnover number $\geq 10^4$–10^6 reactions per second)

(Donaldson and Quinn 1974). The equilibrium of both C_i forms in the solution obeys Henderson–Hasselbalch equation (see Eq. 2.7), and proportion of each form in solution is a function of pH.

$$\mathrm{pH} = \mathrm{pKaH_2CO_3} + \log_{10}\left(\frac{\left[\mathrm{HCO_3^-}\right]}{\left[\mathrm{H_2CO_3}\right]}\right) \tag{2.7}$$

The reaction shifted toward the formation of CO_2 in acidic conditions (pH < 6.4) while HCO_3^- form is prevalent in alkaline conditions (pH ~ 6.4 and 10.3).

(a) Basic structure and mechanism of action

The X-ray crystallographic data of CAs suggest that the zinc containing active site is situated at 15 Å deep cleft and coordinated with three histidines in a distorted tetrahedral geometry and one water/hydroxide molecule (Zn^{II}–H_2O or OH) (Zastrow and Pecoraro 2013). The binding cleft has hydrophobic and hydrophilic faces.

The Fig. 2.5 shows the structural arrangement of CA-II from protein data base (PDB) entry 1CA2 (Eriksson et al. 1988). The active site consists of a zinc prosthetic group, shown with a big red and green sphere. Imidazole rings of highly conserved histidine residues (shown with numbers 94, 96, and 119) directly coordinate with zinc while additional fourth coordination position, shown with small red sphere, occupied by water or hydroxide ion molecule (depending on medium pH).

At this specific pocket, atoms of threonine (Thr_{199}) and glutamate (Glu_{106}) as well as histidine assist to charge the zinc with a hydroxyl ion (Zastrow and Pecoraro 2013). The catalytic site also have affinity compartment for CO_2, bringing it close to the hydroxide group. CO_2 is not coordinated to the Zn^{II} but instead binds weakly ($K_d \approx 100$ mM) at a hydrophobic region (Krishnamurthy et al.

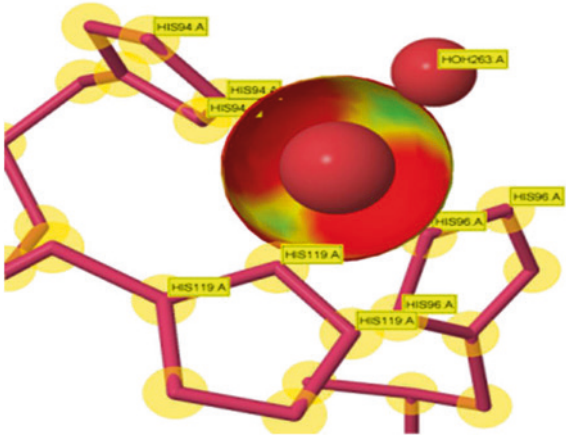

Fig. 2.5 Structural organization of carbonic anhydrase (PDB-1CA2)

2008). Because zinc ion is a positively charged, it stabilizes the negative hydroxyl ion, thus it is prepared to attack the CO_2. Several CA isozymes have variations in these and other residues at active site, which may elucidate in their catalytic activity. Despite significant structural variations at the active sites, all CAs (majorly α- and γ-class) employ zinc hydroxide-binding mechanism (Parkin 2004). The zinc hydroxide-binding mechanism can be divided into four steps.

(i) Step 1: Deprotonation

As a universal feature of all known Zn^{II}-metalloenzymes, the Zn^{II} ion acts as a key element to activate this water molecule for catalysis. In biological machinery, zinc is always found only in the Zn^{+2} oxidation state (Kröncke and Klotz 2009). The chemical reaction of zinc elements linked with their positive charges and their capacity to form strong but kinetically labile bonds in more than one oxidation state (Berg et al. 2002). Core zinc metal helps in the activation of CA via release of a proton from a Zn-bound water (Zn^{II}–OH_2^+) to produce a zinc-bound hydroxide ion (Zn^{II}–OH). The role of the Zn^{+2} is here to lower the pK_a of the bound water molecule from 15.7 to 7, making the oxygen slightly more negative and polarization of hydrogen-oxygen bond. This is important for the mechanism, since the hydroxyl ion bound to Zn^{+2} form is more active than a water molecule.

(ii) Step 2: Carboxylation

Further, Zn^{II}–OH complex is also employed in H-bond interactions through the hydroxyl group of Thr_{199}, which is consecutively bonded with the carboxylate group of Glu_{106} (Kumar et al. 2007). These interactions make Zn^{II}–OH complex a potent catalytically active electron-rich nucleophile, and orient the substrate CO_2 molecule in a favorable position for the nucleophilic attack (Wang et al. 2011). This strong Zn^{II}–OH nucleophile attacks the CO_2 molecule bound in a hydrophobic pocket (substrate-binding site comprises residues Val_{121}, Val_{143}, Val_{207}, Leu_{198}, and Trp_{209} in hCAII) located above and to the right of the active site, leading to the formation of bicarbonate coordinated to Zn^{II}.

(iii) Step 3: Construction of ring-like intermediate complex

This is an intermediate stage in which a bond is created, connecting the hydroxyl ion and the CO_2 molecule. Anionic oxygen of CO_2 molecule forms a bond through core Zn^{II} to build a ring-like resonance.

(iv) Step 4: Regeneration of active form

In the final step, the active site of CA is restored for another round of catalysis. The formed bicarbonate ion is liberated, and one more water molecule binds to center zinc ion (Berg et al. 2002). Addition of water displaced the bicarbonate ion and liberated into solution. It leads to the formation of catalytically inactive acid form of the enzyme, Zn^{II}–OH_2^+. To regenerate the active form, a proton transfer reaction from the active site to the environment takes place, which may be assisted either by active site residues (such as His_{64}) or by buffers present in the medium.

The process may be schematically represented by reactions 1–4 in Fig. 2.6:

(b) Variants of CAs

Over the past decade, importance of CAs proteins and their genes in all domains of living organic world are implied by widespread distribution from prokaryotes such as archaebacteria and eubacteria to eukaryotes such as vertebrates (including humans) (Pastorek et al. 1994), invertebrates (Ferguson et al. 1937), and plants (Badger and Price 1994). The widespread variants of CA enzyme in nature is probably due to the fact that its substrate, C_i, is the most important element involved in all vital cellular processes. The comparison of amino acid sequences of all currently known CAs revealed the fact that they belong to five independent CA gene families, designated as α, β, γ, δ, and ε (Aspatwar et al. 2010). The crystal structures for representatives of α-, β-, and γ-classes have now been determined and shown in Fig. 2.7, while the structures of the recently identified δ- and ε-classes are yet to be solved.

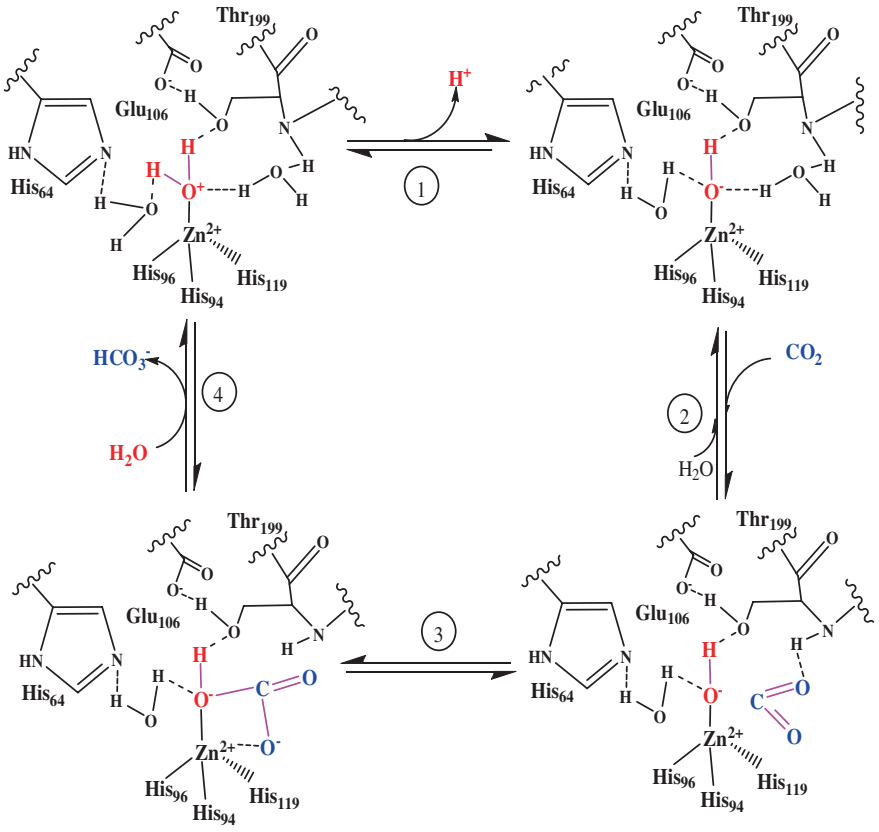

Fig. 2.6 Zinc hydroxide-binding mechanism of carbonic anhydrase

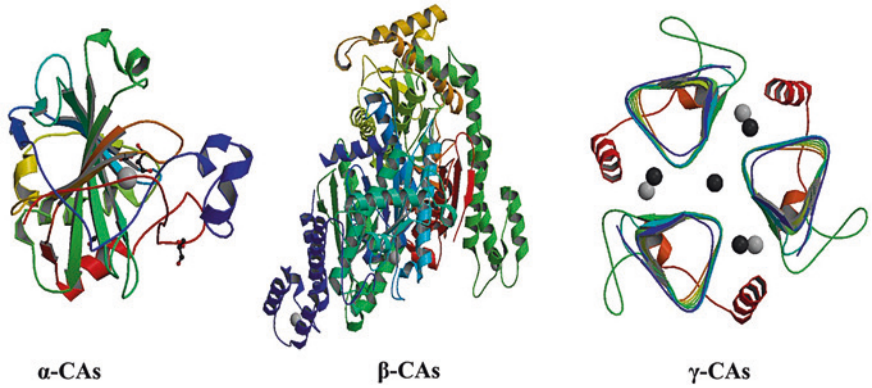

Fig. 2.7 Refined structure of *α-CA* (PDB:1CA2, Eriksson et al. 1988), *β-CA* (PDB:2FGY, Heinhorst et al. 2006), and *γ-CA* (PDB:3KWD, Peña et al. 2010)

All CA enzyme families are of ancient origin and appears to have evolved independently from one another, i.e., no significant homology in amino acid sequence, thereby providing an excellent example of convergent evolution of catalytic function (Supuran 2011). Thus, they have structurally distinct overall folds in the spatial organization of proteins. Yet, despite their structural differences, mechanism of catalysis of the majority of CAs is similar and common for all evolutionary lineages of the enzyme. Metal-containing active centers of all classes function with a single zinc atom that is essential for catalysis.

(i) α-CAs

The α-CAs gene family is the most intensively studied and widely distributed CA family, which considered as the youngest phylogenetic group. The α-class are found predominantly in animals (Boone et al. 2013), but homologs have also been identified in the bacterium *Neisseria gonorrhoeae* (Hiltonen et al. 1998) and the green alga *Chlamydomonas reinhardtii* (Fukuzawa et al. 1990). The active site of α-class has high attraction for Zn, and geometrical organization of conserved histidine residues favors Zn binding. The active site is located at the bottom of a 15-Å-deep active site cleft dominated by hydrophobic amino acid side chains at the base of which is a Zn^{2+} ion invariably coordinated by imidazole rings of three his ligands, His_{94}, His_{96}, and His_{119} (Tetu et al. 2007) and a water molecule/hydroxide ion. To date at least 15 α-CA- or α-CA-like isoforms have been found in mammals, which can be subdivided five broad subgroups as cytosolic CAs (CA-I, CA-II, CA-III, CA-VII, and CA XIII), mitochondrial CAs (CA-VA, and CA-VB), secreted CAs (CA-VI), membrane-associated (CA-IV, CA-IX, CA-XII and CA-XIV), and those without CA activity, the CA-related proteins (CA-RP VIII, X, and XI). In the aquatic photosynthetic organisms such as green alga *Chlamydomonas reinhardtii*, three CA isozymes located at periplasmic glycoproteins have been sequenced, evolutionary related to mammalian CAs (Moroney

et al. 2011). α-CAs typically activated as protein monomers of about 30 kD that are mostly composed of 10-stranded secondary structure, a twisted β-sheet, which separates the α-CA molecules into two halves. Except for two pairs of parallel strands, the β sheet is antiparallel (Liljas et al. 1972).

(ii) β-CAs

The β-CAs are perhaps the most diverse lot of the five currently known CAs, structurally and functionally. The β-CAs were initially identified in chloroplast of higher plants (Burnell et al. 1990; Fawcett et al. 1990) but are now known to be present in various subcellular compartments of microalgae (Eriksson et al. 1996), cyanobacteria (Fukuzawa et al. 1992; Soltes-Rak et al. 1997), eubacteria (Hewett-Emmett and Tashian 1996), archaea (Smith and Ferry 1999), and fungi (Schlicker et al. 2009). Interestingly, β-CA is far more diverse in amino acid sequence than the other two classes, suggesting that they evolved independently. The entire β-CAs share an exclusive α/β fold not exist in any other proteins (Covarrubias et al. 2006). In contrast to α-CAs that is mostly composed of β-sheets, β-CAs contains a number of α-helices. Moreover, β-CAs have only one conserved histidine residue (His $_{205/459}$), whereas α-CAs have three (Supuran and Scozzafava 2007). Unlike α and γ-CAs which form strictly monomers and trimers, β-CAs are only functional when homodimeric active core of β-CA oligomerized as a dimer, tetramer, or octamer depending on the species of origin (Mitsuhashi et al. 2000; Huang et al. 2011). The oligomerization state appears to be motivated by outside extensions or exclusive amplifications of the secondary structure of basic β-CA fold (Kimber and Pai 2000; Krissinel and Henrick 2007). β-CA can adopt a variety of functional oligomeric states with molecular masses ranging from 45 to 200 kD (Mitsuhashi et al. 2000). However, the fundamental active structural unit of β-CAs appears to be a dimer or multimers. Dimerization enables formation of the hydrophobic pocket required for CO_2binding and forms the active site at the interface. Core zinc ion geometry is supported by a combination of cysteine, histidine, and glutamic acid or cysteine again, depending on the species (Mitsuhashi et al. 2000).

The most common arrangement for β-CA is a tetramer (HICA, ECCA, Rv1284) or a pseudo-tetramer composed of two pseudo-dimers (PPCA, HTCA) (Kanth et al. 2012). The extant X-ray crystal structures of β-CA appear to fall into two distinct structural classes as determined by the organization of the active site region in its uncomplexed state, designated here as “Type I β-CA” and “Type II β-CA” (Sawaya et al. 2006). The principal differences between these two types of β-CA relate to the ligation state of the active site zinc ion, and the orientation and organization of nearby residues (Table 2.1).

(iii) γ-CAs

The γ-class may be the most prehistoric form of CAs, having evolved long before the α-class, to which it is more closely related than to the β-class (Badger and Price 2003). The γ-class is also broadly distributed in diverse species from all three domains of life, predominantly in bacteria and archaea domains. A γ-CA was first discovered and isolated in the methanogenic archaebacterium that grow

Table 2.1 Physiological characteristics of Type I β-CA and Type II β-CA

Physiological character	Type I β-CA	Type II β-CA
Coordination sphere for zinc	$Cys_2His(X)$, where X is an exchangeable ligand (e.g., acetate, acetic acid, water)	$Cys_2HisAsp$
Asp–Arg dyad (helps in orient the Asp residue to accept a hydrogen bond from an exchangeable ligand atom bound directly to the Zn^{2+})	Asp–Arg dyad present	A broken Asp–Arg dyad is present
Hydrogen bond donor (for interaction between Zn^{2+} and HCO_3^- ions in the exchangeable ligand position	Hydrogen bond donor present	Hydrogen bond donor absent
Narrow hydrophobic active site cleft that lies along the dimer or pseudo-dimer interface and leads to the active site Zn^{2+} ion	Present	Present

in hot springs *Methanosarcina thermophila* (Alber and Ferry 1994). To date, the only "Cam" (for **CA** of ***M****ethanosarcina thermophila*) has been shown to have CA activity in trimerized form (Kisker et al. 1996). All other Cam homologs from both plants and bacteria, including CcmM from the cyanobacteria *Synechocystis* PCC6803 and *Synechococcus* PCC7942, were found to lack CA activity (Peña et al. 2010). This suggested that these homologs have evolved a different function and that Cam is a relic. They obtain energy for growth by metabolizing acetate to CH_4 and CO_2 (Smith and Mah 1978). The role of γ-CA in acetate metabolism is to drive forward reaction of acetate to methane and CO_2 by removing the CO_2 concentration by converting it to HCO_3^- outside the cell. γ-CAs catalyze the reversible hydration of CO_2 to HCO_3^- ion on opposing sides of the membrane thereby facilitating anion exchange, in order to reduce the concentration of CO_2 produced in acetate metabolism. In the cyanobacterium *Synechocystis*, the bifunctional CcmM protein localized in carboxysome shows an N-terminal γ-CA-like domain, which has been proposed to bind HCO_3^-/CO_2 (Cot et al. 2008). Recent work has indicated that γ- or γ-like CAs are part of Complex I of the mitochondrial electron transport chain in plants and algae (Wang et al. 2012).

According to the structural classification of proteins (SCOP), γ-CA is part of the Trimeric LpxA Enzyme superfamily, which is characterized by single-stranded polypeptides with left-handed beta-helix fold. Cross-sectional profiles of the γ-CA trimer reveal that each left-handed beta-helix monomer structure resembles an equilateral triangle complex (Iverson et al. 2000). The beta-helix consists of three untwisted, parallel sheets that are connected by left-handed crossovers. The active sites are located at the interfaces between two β-helices. The interface is stabilized by H-bonds, salt bridges, and hydrophobic interactions. The trimer contains 3 active sties, and each monomer contributes His residues located on the surface to coordinate with the 3 zinc ion, Zn^{2+} or the cobalt ion, Co^{2+} (Kisker et al.

1996), and one at each subunit interface. The unique feature of γ-CA is its ability to utilize both metal ions equivalently for its active site, depending on their availability. There are no significant differences between both forms (zinc-bound and cobalt-bound γ-CA) structures and their catalytic mechanism for carbon dioxide hydration reaction. Both have three histidine residues (His_{81}, His_{117}, and His_{122} residues) that coordinate the ion with the active site (Tripp et al. 2001). In addition to His, there are several other residues which have been identified to play an important role in the active site catalytic mechanism. For example, glutamine (Gln_{75}) and asparagine residues (Asn_{73}) have been found to help orient Co^{2+} ion for attack on the CO_2, and asparagine residue (Asn_{202}) prepares the CO_2, by polarization, for attack by the Co^{2+} ion. The reaction mechanism of the γ-class is similar to that of the α-class, even though, overall folds and active site residues are different (apart from those that ligand the zinc).

(iv) δ-CAs

A fourth class of CA named δ-class has been isolated from the marine diatom *Thalassiosira weissflogii* (Roberts et al. 1997). X-ray absorption spectroscopy of the δ-CA, *T. weissflogii* CA1 (TWCA1), has shown that it indeed does contain a Zn^{2+} ion bound by histidine residues. Presently, there are only 4 other proteins that display amino acid sequence similarity to TWCA1, and thus, its distribution may be restricted to only a small number of diatom species (So and Espie 2005).

(v) ε-CAs

The fifth epsilon class of CAs occurs exclusively in bacteria containing α-type carboxysomes in a few chemolithotrophic bacterium *Halothiobacillus neapolitanus,* hydrogen bacteria and many strains of marine cyanobacteria that contain CsoS3-carboxysomes (So et al. 2004; So and Espie 2005). X-ray 3-D crystal structure analyses of *H. neapolitanus* suggest that active site of ε-CA bears some structural resemblance to β-CA (Sawaya et al. 2006) particularly near the metal ion site with a histidine and two cysteine residues acting as zinc ligands, in spite of the absence of any primary sequence similarity. This suggested that CsoS3 is a subclass of β-CA comes from the striking structural similarity of the Zn^{2+}-containing active site and from the fact that both need to form dimers in order to be active (Sawaya et al. 2006). In all examples to date, CsoS3 is encoded within the Cso operon which encodes all the components for the α-carboxysome (Rae et al. 2013). Thus, the two forms may be distantly related, even though the underlying amino acid sequence has since diverged considerably. This class of CA has not been found in eukaryotes.

2.3.2.3 RuBisCO Micro-Compartment System

A third basic requirement of a CCM is the existence of effective RuBisCO-rich micro-compartment system, essential for fixing and minimizing the leakage of CO_2 (Price et al. 2008). RuBisCO is commonly, catalyzes the first rate limiting

step within the Calvin cycle (Berg et al. 2002). RuBisCO has a large active site that can accept both CO_2 and O_2 as a substrate (van Lun et al. 2014). O_2 has a higher affinity for the active site and therefore will bind at a higher rate than CO_2 , decreasing the carbon fixation ability of RuBisCO. Photosynthetic microorganisms have developed small vesicles within the cell that have tightly packed and concentrated levels of RuBisCO molecules within proteinaceous shell of a specific structure known as the carboxysome (cyanobacteria) or pyrenoid (eukaryotic microalgae) (Mukherjee 2013). The CO_2 is shuttled from outside environment into the proteinaceous shell to maximize the concentration exposure to RuBisCO. We will discuss details of these proteinaceous shells in consequential chapters of the brief.

RuBisCO: Nature's CO_2-Sequestering Enzyme

RuBisCO (Ribulose-1,5-bisphosphate carboxylase/oxygenase, E.C.4.1.1.39), the most abundant protein on Earth (Ellis 1979), forms a bridge in between living biological system and the lifeless chemical network via converting inorganic of the air to organic carbon. It is believed that nearly all of the carbon atoms that are present in living organisms have passed through the active site of RuBisCO, as 95 % of all carbon fixations by C_3 organisms (that includes all phytoplankton) occur via RuBisCO (Raven 1997). RuBisCO occurs universally in most autotrophic organisms from prokaryotes (photosynthetic and chemoautotrophic bacteria, cyanobacteria and archaea) to eukaryotes (various algae and higher plants) on land and in the ocean (Andersson 2008). Since, it constitutes up to 50 % of the soluble protein in the leaf of C_3 plants and ~30 % in C_4 plants (Spreitzer and Salvucci 2002; Sugiyama et al. 1984), considered an extremely important enzyme ecologically, agriculturally, and industrially. Due to the importance and abundance of RuBisCO, aspects of the genetics, microbiology, molecular biology, biochemistry, and evolution of the enzyme have been studied intensely.

Molecular Forms of RuBisCO

The first RuBisCO structure to be solved was that from the bacterium *Rhodospirillum rubrum* (Andersson et al. 1989; Schneider et al. 1990). Further studies by many researchers (Portis 1992; Newman and Gutteridge 1993; Taylor and Andersson 1997; Sugawara et al. 1999; Tabita 1999; Portis 2003; Warlick 2013) have shown that all RuBisCOs found in nature are comprised of two types of polypeptide subunits: a large subunit (L) of 50–55 kD and a small subunit (S) of 12–16 kD (Andersson 2008). On the basis of their number, presence or absence, and structural arrangement, RuBisCOs can be classified into four different molecular forms designated as form I, II, III, and IV (Tabita et al. 2007) (see Fig. 2.8). These multimeric forms have often distinctive features; however the primary structural motif, frequent to every holoenzyme forms, is the catalytic large

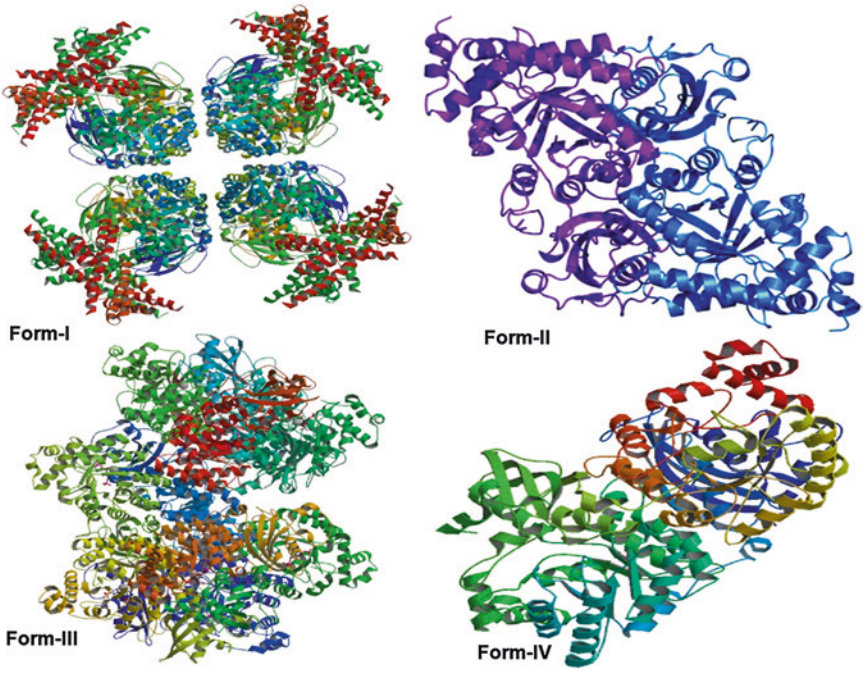

Fig. 2.8 Structure of RuBisCO forms; *form I* (Bracher et al. 2011), *form II* (Tabita et al. 2008), *form III* (Nishitani et al. 2010), and *form IV* (Tabita et al. 2007)

subunit dimer (Tabita et al. 2008). The most abundant form of RuBisCO, Form I is comprised of 8 small and 8 large subunits. The fundamental catalytic structural unit, the dimer of L, is polymerized 4 times to form a core (L_8) of 8 L subunits, with small subunits on top and bottom of this core (Saschenbrecker 2007; Saschenbrecker et al. 2007; Tabita et al. 2008). It is found in plants, algae and cyanobacteria and some members of α-, β- and γ-proteobacteria. Further categorization of form I of RuBisCO contains IA and IB forms (green-type enzymes from cyanobacteria, eukaryotic algae, and higher plants) and IC and ID forms (red-type enzymes from non-green algae and phototropic bacteria) (Tabita et al. 2008). Form II is composed of only the large subunit and is present in dinoflagellates and some members of α-, β- and γ-proteobacteria. Interestingly, the phototrophic purple non-sulfur bacteria (e.g., *Rhodobacter sphaeroides*, *Rhodobacter capsulatus*) and other organisms including *Hydrogenovibrio marinus* and some *Thiobacillus* species contain both form I and form II RuBisCO, and in *R. capsulatus* both forms are expressed under photoautotrophic conditions (Badger and Bek 2008). Form III is found in archaea and consists of a large subunit in a dimeric or pentameric arrangement (Andersson 2008). Form IV is referred to as the RuBisCO-like protein (RLP) because it does not catalyze bonafide RuBisCO CO_2/O_2 fixation reactions by using RuBP as the substrate (Hanson and Tabita 2001). Even though

the RLPs do not seem to be functionally related to RuBisCO, they do, however, share a common sequence identity but do not maintain some key residues present in RuBisCO that are required for catalytic activity. Thus, one may speculate that the lack of these key residues is the reason for RLP's inability to catalyze the RuBisCO CO_2/O_2 bonafide reaction.

It has been suggested that photosynthetic RuBisCO evolve distinct forms of RuBisCO in nature; form I, II, III, and RuBisCO-like form IV based on amino acid sequences, phylogeny, and structure (Tabita et al. 2007; Andersson and Backlund 2008). An important structural difference between the form I/II and form IV subfamilies lies in loop 6 in which the Lys334 of the photosynthetic RuBisCOs is generally substituted by another amino acid residue (Carrae-Mlouka et al. 2006).

Structural Arrangement of RuBisCO

Numerous high-resolution crystal structures of different forms of RuBisCO are now available which provide a molecular framework for the understanding of structural arrangement of RuBisCO at the molecular level. On the basis of available facts, it is now believed that the fundamental catalytic structural unit of all RuBisCOs is common to all forms, usually consists of two distinct catalytic subunits; large catalytic subunits (L, about 55 kD each) and small subunits (S, about 15 kD each) (Andersson 2008). In form I RuBisCO, eight copies each of two distinct subunits are cemented to form quaternary structure of about 560 kD molecular mass for the complete protein (L_8S_8) superstructure (Bracher et al. 2011). The 8L subunits of form I are arranged as an octameric core surrounded by two layers of four S subunits, with each layer located on opposite sides of the molecule. A Mg^{2+} cofactor as well as the carbamylation of Lys_{201} is also required for the activity of the enzyme (Tabita et al. 2008).

Genes for RuBisCO

The clustering of genes (e.g., *rbcL*, *rbcX,* and *rbcS*) is thought to assist in coding for the structurally related various complex components synthesis and assembly (Tabita 1999) of CO_2-fixing hexadecameric (L_8S_8) RuBisCO enzyme. For synthesis of the functional RuBisCO holoenzyme in microalgae, eight identical large subunits encoded by the chloroplast gene *rbcL* and eight identical, small subunits encoded by the nuclear gene *rbcS* (Clegg et al. 1997). Within cyanobacteria, both genes are adjacent and co transcribed.

(a) *rbcL*

Despite variations in the amino acid sequences (average amino acid sequence identity is 31 %), the overall secondary structural motifs of the large (catalytic) subunit shares similarities and well conserved within all forms of RuBisCO super

family (Tabita et al. 2007). *rbcL* expression may be regulated by the epistasy of synthesis (CES) paradigm, in which unassembled L-subunit motifs connect to mRNA of *rbcL* to autoregulate its translation (Whitney et al. 2011). Large subunits within RuBisCO are arranged as antiparallel dimers, with the smaller N-terminal domain (4–5 stranded mixed β sheet) of one monomer adjacent to the C-terminal domain (8 consecutive β–α units) of the other monomer (Tabita et al. 2007). Each active site is at an interface between monomers within an L_2 dimer, explaining the minimal requirement for a dimeric structure. The β–α units of C-terminal, are linked by many loops of different length and arranged as an eight stranded parallel α/β barrel structure, which act as a evolutionary markers and directed evolution techniques to engineer novel catalytic activities (Vega et al. 2003). The substrate-binding site is at the intra-dimer ($RbcL_2$) interface on the mouth of a α/β-barrel domain of the large subunit, linking the C-terminal domain of the one large subunit (β-strands) and the N-terminal domain of the second large subunit. Consequently, the functional unit configuration of RuBisCO is an L_2 dimer of large subunits harboring two active sites. The substrate binds in an extended conformation across the opening of the α/β barrel and is secured at two distinctive phosphate-binding sites at reverse sides of the α/β-barrel and in the center at the Mg^{2+} cofactor-binding site (Tabita et al. 2007). Most catalytic residues at enzyme active site are polar, including some charged amino acids (e.g., Thr, Asn, Glu, and Lys) (Bartlett et al. 2002).

(b) *rbcS*

Small subunits are not necessary for the assembly of the $RbcL_8$ core. However, availability of *rbcS* (13.3 kD) protein up-regulates the gene expression of *rbcL* primarily at the transcript level in a quantitative manner for stoichiometric assembly of RuBisCO holoenzyme (Morita et al. 2014). It is tempting to speculate that the small subunits contribute substantially to the differences in kinetic properties observed among different RuBisCO enzymes. In eukaryotic microalgae, small subunits are probably encoded by the *rbcS* multigene family in the nuclear genome (Clegg et al. 1997). It is believed that mRNA of *rbcS* has been laterally transferred from the ancestral plastid's genome to become a nuclear multigene family (Whitney and Andrews 2001). They have a transit peptide, bearing an amino-terminal targeting signal, which helps small subunit precursor proteins to be imported and assembled into the chloroplasts after translation on cytosolic ribosomes, where they are processed and folded to the native state (Flores-Paerez and Jarvis 2013). Whereas, the large subunits display relatively small variations in the different forms, the small subunit is more diverse. The small subunits help to sustain the catalytic competence and structural integrity of $RbcL_8S_8$ holoenzyme by establishing prevailing links among the four $RbcL_2$ dimers (Windhof 2011, Liu et al. 2010). The common core structure of small subunits consists of a four-stranded antiparallel β-sheet covered on one side by two helices. Among the form I RuBisCOs, most striking variations occur in two distinct locations, the small subunits differ in between β strands A and B of small subunit, called βA–βB loop (Andersson 2008).

(c) *rbcX*

In contrast to eukaryotes, most prokaryotes such as cyanobacteria, the gene *rbcX* (~15.5 kD) is present between *rbcL* and *rbcS* and co-transcribed with the *rbcL* (52 kD) and *rbcS* genes on the same operon (Larimer and Soper 1993). Previous co-expression studies showed that *rbcX* product of the intermediary *rbcX* gene is not part of the final RuBisCO complex and unlike *rbcL* and *rbcS* whose sequences are highly conserved by functional constraints. The *rbcX* sequence is highly variable (<60 % similarity) among cyanobacterial species (Rudi et al. 1998). However, recent evidence suggests that juxtaposition of *rbc*X within an *rbc*LXS operon is highly conserved in β-cyanobacteria, recommending that the *rbcX* product may function in a role associated with CO_2 fixation (Emlyn-Jones et al. 2006; Saschenbrecker 2007; Saschenbrecker et al. 2007; Onizuka et al. 2004).

Reaction Mechanism of RuBisCO

RuBisCO is most commonly known to a bifunctional enzyme that occurs in the stroma of chloroplasts and catalyzes both carboxylation and oxygenation reactions (Tabita et al. 2008). These reactions are the basis for the name RuBP carboxylase/oxygenase (RuBisCO). In order for RuBisCO to function, it requires substrates supplied from the surrounding environment. In these reactions, both CO_2 and O_2 substrates compete for the same active site on RuBisCO to drive photosynthesis and photorespiration, respectively. Both metabolic routes are found in most autotrophic organisms, ranging from prokaryotes (cyanobacteria and other phototrophic and chemoautotrophic bacteria) to eukaryotes (various algae and higher plants) (Spreitzer et al. 2002).

(a) *Carboxylation*

When CO_2 is the substrate gathered in specific location of the RuBisCO, it performs a conformation change and catalyzes the carboxylation reaction with the activation of RuBP carboxylase. Carboxylation involves the fixation of one molecule of CO_2 with a molecule of five-carbon sugar substrate, ribulose-1,5-bisphosphate (RuBP) to produce a highly unstable six-carbon reaction intermediate (Blankenship 2014). Due to the intermediate molecules instability, carbon splits into two molecules of 3-phosphoglycerate (3PGA). This reaction occurs in several partial reactions (Karkehabadi 2005) (see Fig. 2.9).

- Enolization—Enzymatic abstraction of a proton (H^+) from C-3 of the RuBP substrate results in the formation of the 2,3-enediol intermediate (I). Mg^{+2} aids in stabilizing the 2,3-enediol transition state for CO_2 addition and facilitates the C–C bond cleavage that leads to two 3-C products.
- Carboxylation—The addition of CO_2 at C-2 to create a 6-carbon β-keto acid intermediate (II), 2-carboxy-3-keto-arbinitol-1,5-bisphosphate (CKABP).

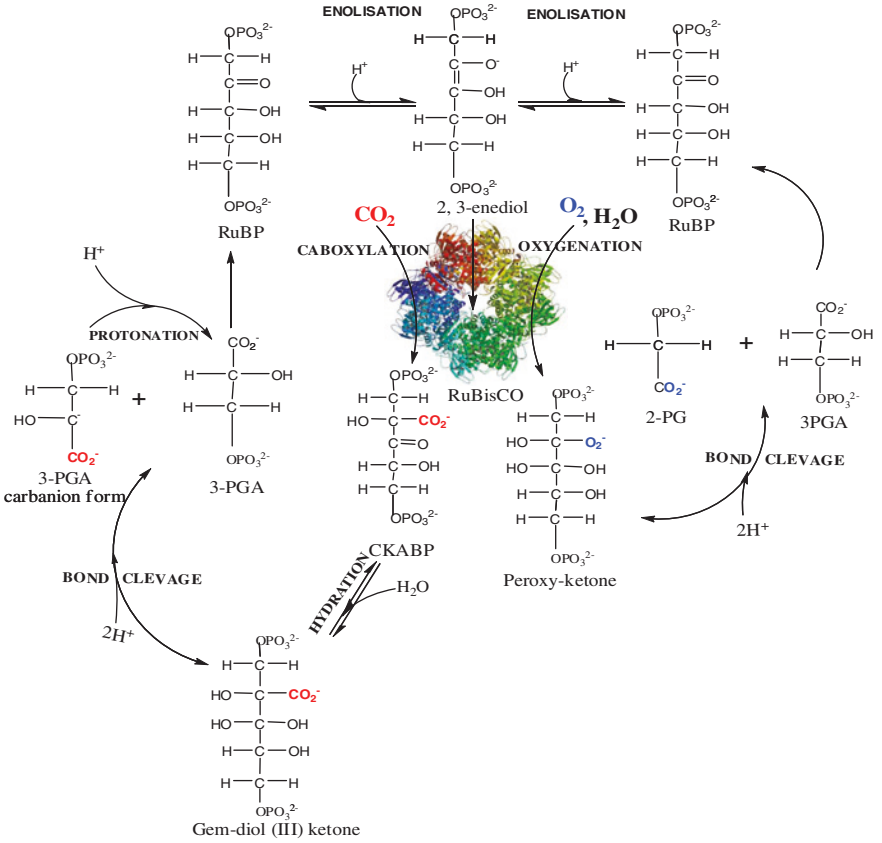

Fig. 2.9 RuBisCO pathways for carboxylation and oxygenation

- Hydration—The hydration of CKABP yields the gem-diol (III) form of the ketone.
- Deprotonation—Deprotonation at C-3 hydroxyl of the gem-diol (III) leads to C–C bond cleavage and results in formation of one molecule of 3-phosphoglycerates (3PGA) and one molecule of 3-PGA in the form of carbanion.
- Protonation—The carbanion is protonated, and the second molecule of 3-PGA is formed.

(b) *Oxygenation*

When molecular O_2 is the substrate, RuBisCO catalyzes the oxygenation of sugar substrate RuBP to yields one molecule each of 3PGA and 2-phosphoglycolate (Karkehabadi 2005). The phosphoglycolate has very limited use in most organisms

and needs to be re-circulated through the sequence of complex energy-requiring reactions called C-2 photosynthesis or photorespiration that partly salvages carbon from 2-phosphoglycolate, via conversion to 3-phosphoglycerate, involves enzymes of chloroplasts, peroxisomes, and mitochondria. This pathway recovers 3/4 of the carbon from 2-phosphoglycolate as 3-phosphoglycerate while the rest is released as CO_2. As photorespiration consumes ATP and reducing power, while losing CO_2, before it is converted to PGA and reenters to the metabolic pathways for carbon fixation (Laing et al. 1974). It is consider a wasteful process which substantially reduces the efficiency of CO_2 fixation by up to 50 % (Ogren 1984). Thus, the incapability of the RuBisCO to avoid the reaction with O_2 greatly reduces the photosynthetic capacity of photosynthetic organism. It would appear that eliminating or reducing the RuBisCO oxygenase activity would potentially increase carbon assimilation, thereby rising photosynthetic efficiency significantly (McGrath and Long 2014). Many algae and photosynthetic bacteria have conquered this restriction by devising means to raise the CO_2 concentration around the enzyme through carbon-concentrating mechanism.

2.4 Fate of Carbon in Photosynthetic Microorganisms

Although CO_2 occurs in small amounts in the atmosphere, it has a considerable impact on living organisms, since it is a key substrate of photosynthesis. The aquatic environment is home of diversity of photosynthetic pathways as terrestrial environments, and therefore, photosynthetic organisms reduce CO_2 via various carbon fixation mechanisms, C_3, C_4, CAM, and C_3–C_4 photosynthetic pathways (Xu et al. 2012). Reduction takes place in in the stroma, or soluble phase, of chloroplasts, coupled to the consumption of NADPH and ATP synthesized by the light reactions of thylakoid membranes (Blankenship 2014). Here, CO_2 and water are combined with ribulose-1,5-bisphosphate to form two molecules of 3-phosphoglycerate. Phosphoglycerates are familiar molecules in the cell, and many pathways are available to use it to produce larger biomolecules such as carbohydrate. Most of the phosphoglycerate made by RuBisCO is recycled to build more ribulose bisphosphate, which is needed to feed the carbon-fixing cycle. The continued operation of these cycles is ensured by the regeneration of ribulose-1,5-bisphosphate. From many studies on primary photosynthetic carbon metabolism, it is believed that the operation of the Calvin–Benson cycle (C_3 cycle) is predominant in algae and cyanobacteria. However, recent papers have also reported evidence for the operation of C_4 photosynthesis and both C_3 and C_4 fixation in some species, as an alternative CCM. Alterations of photosynthetic pathways under environmental stress such as CO_2 deficiency have been suggested to contribute to the adaptation of photosynthetic organisms to environmental stress. The major physiological differences between C_3 and C_4 cycles are tabulated in Table 2.2.

Table 2.2 Physiological differences between C_3 and C_4 cycles

Property	C_3 cycle	C_4 cycle
CO_2 molecule acceptor	Ribulose bisphosphate	Phosphoenol pyruvate
First stable product	Three-carbon compound 3-phosphoglycerate (3PGA)	Four-carbon compound 3-oxaloacetic acid (OAA)
Photorespiration rate	High and leads to loss of fixed CO_2	Negligible or almost absent
Optimum temperature	20–25 °C	30–45 °C

2.4.1 C_3 or Calvin–Benson–Bassham Cycle

A majority of photosynthetic organisms assimilate CO_2 via a set of redox reactions, C_3 pathway (Calvin–Benson–Bassham cycle) that occurs without light during photosynthesis (Björn 2008). The cycle was elucidated about 50 years ago as a result of a series of elegant experiments by Calvin, Bassham, and Benson at the University of California, Berkeley, for which a Nobel Prize was awarded in 1961 (Calvin et al. 1950). They used radioactive $^{12}CO_2$ isotopes to reveal the path of carbon atoms taking place in unicellular green alga *Chlorella pyrenoidosa,* during the transformation of CO_2 into carbohydrates. The C_3 cycle utilizes the high-energy products of light-dependent reactions, ATP and NADPH, to fix atmospheric CO_2 into carbon compounds that are used to fuel the rest of plant metabolism (Whitmarsh 1999). The carbon in CO_2 is the most oxidized form, (+4) oxidation state, found in nature. With 4 valence shell electrons, carbon tends to form covalent compounds. Thus, first stable intermediate, 3-phosphoglycerate of the C_3 cycle, is more reduced (+3) and after it is further reduced to glyceraldehyde-3-phosphate (+1) product (Blankenship 2014). Therefore, early reactions of the C_3 cycle complete the reduction of atmospheric carbon and, in so doing, facilitate its incorporation into organic compounds. This cycle operates in plants, algae, cyanobacteria, some aerobic or facultative anaerobic proteobacteria, CO_2-oxidizing mycobacteria, and representatives of the genera sulfobacillus (iron- and sulfur-oxidizing firmicutes) and Oscillochloris (green sulfur bacteria) (Whitmarsh 1999). The Calvin cycle occurs in three stages as shown in Fig. 2.10: carboxylation of RuBP, reduction of 3-phosphoglycerate, and regeneration of RuBP.

2.4.1.1 Carboxylation of Ribulose Bisphosphate

The CO_2 molecules enter in the cycle by reacting with CO_2 acceptor RuBP to yield the first stable intermediate of the cycle, two molecules of 3-phosphoglycerate (3-PGA), reaction catalyzed by the enzyme RuBisCO (Kirk 1994). It is this 3-C molecule, the first stable product of the carboxylation reaction of RuBisCO that gives the C_3 cycle its name. The affinity of RuBisCO for CO_2 is sufficiently high to ensure rapid carboxylation at the low concentrations of CO_2 found in photosynthetic cells.

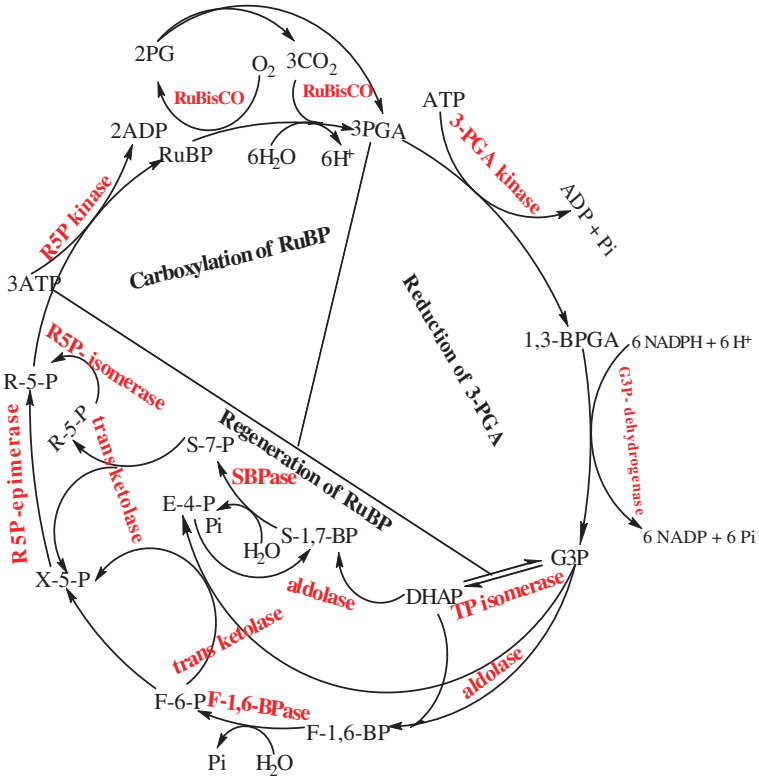

Fig. 2.10 Stages of Calvin cycle

2.4.1.2 Reduction of 3-Phosphoglycerate

The 3-phosphoglycerate formed in the carboxylation stage undergoes reductive phase of the cycle follows with two modifications:

i. The 3-PGA is first phosphorylated catalyzed by 3-PGA kinase to 1,3-bisphosphoglycerate (1,3-BPGA) through use of assimilatory power, ATP, produced in the light reactions.
ii. Further, 1,3-BPGA is reduced to glyceraldehyde-3-phosphate (G-3-P), i.e., carboxyl group is transformed into an aldehyde group, through utilization of the NADPH produced by the light reactions, enzyme NADP: glyceraldehyde-3-phosphate dehydrogenase (GAPDH) catalyzes this step.

2.4.1.3 Regeneration of Ribulose-1,5-Bisphosphate

In order to keep the cycle functioning in the fixation of CO_2 in C_3 pathway, it is essential that necessary biochemical intermediates; CO_2 acceptor, RuBP, etc., be constantly regenerated. To prevent depletion of RuBP, G-3-P enters in the various

sequential reactions of regenerative phase to ensure adequate supply of CO_2 acceptor. All steps of regeneration are summarized as follows:

1. One molecule of G-3-P is converted with the action of triose phosphate isomerase (TP isomerase) to dihydroxy-acetone-3-phosphate (DHAP) in an isomerization reaction.
2. DHAP then undergoes aldol condensation with a second molecule of G-3-P, a gluconeogenesis reaction catalyzed by aldolase to form fructose-1,6-bisphosphate (F-1,6-BP).
3. F-1,6-BP occupies a key position in the regeneration cycle and is hydrolyzed using enzyme fructose-1,6-bisphosphatase (F-1,6-BPase) to fructose-6-phosphate (F-6-P), which then reacts with the enzyme transketolase.
4. A 2-C unit (from C_1 and C_2 position) of donor F-6-P is transferred via transketolase to a third molecule of G-3-P acceptor to give erythrose-4-phosphate (E-4-P) and xylulose-5-phosphate (X-5-P).
5. Further, another aldol condensation via aldolase occurs between E-4-P and a fourth molecule of triose phosphate to yield the 7-C sugar sedoheptulose-1,7-bisphosphate (S-1,7-BP).
6. The S-1,7-BP is sequentially hydrolyzed by dephosphorylation at the C_1 position with the help of phosphatase (SBPase) to give sedoheptulose-7-phosphate (S-7-P).
7. The S-7-P donates a 2-C unit to the last 5th one molecule of G-3-P via transketolase enzyme and forms ribose-5-phosphate (R-5-P) and xylulose-5-phosphate (X-5-P).
8. The two molecules of X-5-P epimerized the C_3 position to form two molecules of R-5-P sugars by enzyme ribulose-5-phosphate epimerase (R5P-epimerase). The third molecule of R-5-P is isomerized to form R-5-P by ribose-5-phosphate isomerase (R5P-isomerase).
9. Finally, ribulose-5-phosphate kinase (R-5-P kinase) catalyzes the phosphorylation at the C_1 position of R-5-P with ATP thus regenerating the three essential molecules of the initial CO_2 acceptor, RuBP (total 15-C) by reactions that reshuffle the carbons from the five molecules of triose phosphate ($5 \times 3 = 15$ C).

Thus, the entire C_3 cycle consumes two molecules of NADPH and three molecules of ATP for every molecule of CO_2 fixed into hexose or carbohydrate (Falkowski and Raven 1997).

2.4.2 C_4 Cycle or Hatch–Slack Pathway

Apart from classical C_3 pathway, Hatch and Slack (1966) reported a new C_4 photosynthesis pathway of CO_2 fixation in sugar cane, which gives an initial four-carbon compound, oxalacetate, rather than 3-PGA. Although timing is uncertain, it is currently thought that C_4 pathway evolved gradually from C_3 ancestors (30 million years ago) through structural and biochemical modifications, in relation to

environmental pressures (e.g., slumping ambient CO_2 level) (Xu et al. 2012). In order to evade the waste photorespiration pathway, C_4 plants possess an additional cytosolic carbon-fixing enzyme phosphoenolpyruvate carboxylase (PEP carboxylase) in addition to RuBisCO (Furbank and Taylor 1995; Chollet et al. 1996). The PEP carboxylase has a higher affinity for CO_2 (lower K_m) and lower affinity for O_2 (higher K_m) than RuBisCO (Sage 2002). Thus, PEP carboxylase is able to fix CO_2 at relatively low intracellular CO_2 concentration. C_4 plants are believed to have evolved gradually from C_3 plants through several intermediate stages of C_3–C_4 plants (Xu et al. 2012). It was also noted that C_4 plants usually show only small or even no apparent CO_2 loss in light. The explanation lies in their unique anatomy (called Kranz anatomy) (Kennedy 1976) and multiple carboxylation reactions. The C_4 terrestrial plants use a ring of specialized cells, bundle sheath cells, for more efficient C_3 carbon fixation, equipped with a CO_2-concentrating mechanism that supports carboxylation of ribulose-1,5-bisphosphate over oxygenation reactions.

As shown in Fig. 2.11, the primary step of C_4 cycle is the production of 3 carbon phosphoenolpyruvate (PEP) from pyruvate using enzyme pyruvate orthophosphate dikinase (PPDK, E.C. 2.7.9.1), inorganic phosphate, and ATP. The next step is the CO_2 fixation through irreversible β-carboxylation of phosphoenolpyruvate (PEP) to 4-carbon oxaloacetate (first stable product) in the presence of ubiquitous

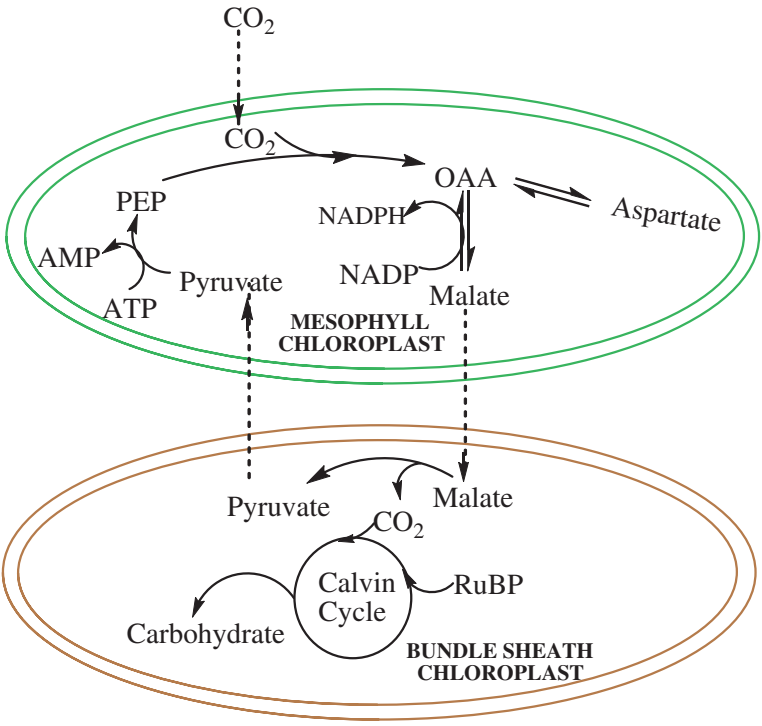

Fig. 2.11 Schematic representation of Hatch–slack pathway

enzyme PEP carboxylase, bicarbonate ions, and Me^{2+} (Furbank and Taylor 1995). Both steps occur in the mesophyll cells. Further, oxaloacetate can be reduced quickly to four-carbon malate using enzyme malate dehydrogenase in the leaf mesophyll cells. Malate is easily transferred to bundle sheath cells and converted to 3 carbon pyruvate, releasing CO_2 and reducing NADP to NADPH for C_3 cycle. This maintains CO_2 concentration high, so that RuBisCO is used almost entirely as a carboxylase, minimizing photorespiration. Thus, PEP carboxylase activity helps to refix any respired CO_2 formed from the oxygenase function of RuBisCO to prevent the photorespiratory release of CO_2.

Although, surprisingly lacks of Kranz dual-cell compartmentation in aquatic photosynthetic microorganisms, recent metabolic labeling and genome sequencing data suggest that the some species including green alga (*Chara contraria, Ostreococcus tauri,* and *Micromonas*) and diatoms (*Thalassiosira weissflogii*, *Phaeodactylum tricornutum,* and *T. pseudonana*) could also use the maneuver of both C_3 and C_4 fixation (Keeley et al. 1986; Keeley 1998; Derelle et al. 2006; Haimovichae Dayan et al. 2013). Presence of C_4 fixation has been further strengthened by the occurrence of relevant genes in their genomes. *Ostreococcus* has all the machinery; PEP carboxylase, $NADP^+$-dependent malic enzyme, and pyruvate orthophosphate dikinase with a predicted chloroplast-targeted transit peptides in a later two, necessary to perform C_4 fixation (van Ooijen et al. 2012). Interestingly, only one member of the marine Chlorophyta, macroscopic green macroalga *Udotea flabellum,* has been shown to perform C_4 photosynthesis (Reiskind and Bowes 1991). It shows that *U. flabellum* utilizes PEP carboxykinase (PEPCK) (as $NADP^+$-malic enzyme being absent), which activity in *Udotea* extracts is equivalent to RuBP carboxylase (Reiskind et al. 1988; Reiskind and Bowes 1991). Recently, the coexistence of genes necessary for both C_3 and C_4 pathway enzymes has also been reported in another green-tide-forming macroalga, *Ulva prolifera* (Xu et al. 2012). The expression levels of C_3 and C_4 photosynthesis genes, *rbc*L and PPDK, increased under stress conditions (such as high and low salinity, high and low temperature). However, contradictory experimental facts of Kremer and Kuppers (1977) shedded doubt on C_4 photosynthesis in algae. They investigated short-term (2–5 s) photosynthesis using $H^{14}CO_3^-$ in various species of different algal classes. *Ulva* produces malate and aspartate organic acids only as a minor component of short time ^{14}C-labeling fixation (less than 10 % of the total ^{14}C-labeling), while RuBP carboxylase (E.C. 4.1.1.39) was the main carbon-fixing enzyme. Usually, aquatic plants are subjected to much lower pCO_2 for photosynthesis. Thus, environmental stress may act as a major driving force to develop alterations of photosynthetic pathways toward C_4 metabolism for suppression of photorespiration. As another example, a submerged aquatic monocot plant *Hydrilla verticillata* operates a facultative, single-cell C_4 system (Rao et al. 2006), i.e., capable to change its photosynthetic pathway from C_3 to C_4 under conditions of CO_2 deficiency. However, studies of photosynthetic pathways of photosynthetic microorganisms are scanty, and there are extremely restricted knowledge of the pathways, which regulating the biology of the altered aquatic C_4 species. Thus, general occurrence of C_4-like mechanisms in aquatic photosynthetic

microorganisms is therefore still in question. Despite its additional energetic cost, if photosynthetic microorganisms are capable of C_4 photosynthesis, it could comprise of a significant ecological benefit in CO_2-limiting conditions of phytoplankton blooms, particularly in conditions where competitors have inferior CCM efficiencies (or no CCM).

References

Alber BE, Ferry JG (1994) A carbonic anhydrase from the archaeon *Methanosarcina thermophila*. Proc Natl Acad Sci 91(15):6909–6913

Andersson I (2008) Catalysis and regulation in RuBisCO. J Exp Bot 59(7):1555–1568

Andersson I, Backlund A (2008) Structure and function of RuBisCO. Plant Physiol Biochem 46(3):275–291

Andersson I, Knight S, Schneider G, Lindqvist Y, Lundqvist T, Branden C-I, Lorimer GH (1989) Crystal structure of the active site of ribulose-bisphosphate carboxylase. Nature 337:229–234

Aspatwar A, Tolvanen MEE, Parkkila S (2010) Phylogeny and expression of carbonic anhydrase-related proteins. BMC Mol Biol 11(1):25

Badger MR, Bek EJ (2008) Multiple RuBisCO forms in proteobacteria: their functional significance in relation to CO_2 acquisition by the CBB cycle. J Exp Bot 59(7):1525–1541

Badger MR, Kaplan A, Berry JA (1980) Internal inorganic carbon pool of *Chlamydomonas reinhardtii*: Evidence for a carbon dioxide-concentrating mechanism. Plant Physiol 66(3):407–413

Badger MR, Price GD (1994) The role of carbonic anhydrase in photosynthesis. Annu Rev Plant Biol 45(1):369–392

Badger MR, Price GD (2003) CO_2 concentrating mechanisms in cyanobacteria: molecular components, their diversity and evolution. J Exp Bot 54(383):609–622

Barber J (2003) Photosystem II: the engine of life. Q Rev Biophys 36(01):71–89

Barsanti L, Gualtieri P (2014) Algae: anatomy, biochemistry, and biotechnology. CRC press, Boca Raton

Bartlett GJ, Porter CT, Borkakoti N, Thornton JM (2002) Analysis of catalytic residues in enzyme active sites. J Mol Biol 324(1):105–121

Berg JM, Tymoczko J, Stryer L (2002) Biochemistry making a fast reaction faster: carbonic anhydrases

Björn LO (2008) The evolution of photosynthesis and its environmental impact. In: Photobiology. Springer, pp 255–287

Blankenship RE (2014) Molecular mechanisms of photosynthesis. Wiley

Boone CD, Habibzadegan A, Gill S, McKenna R (2013) Carbonic anhydrases and their biotechnological applications. Biomolecules 3(3):553–562

Bracher A, Starling-Windhof A, Hartl FU, Hayer-Hartl M (2011) Crystal structure of a chaperone-bound assembly intermediate of form I RuBisCO. Nat Struct Mol Biol 18(8):875–880

Burnell JN, Gibbs MJ, Mason JG (1990) Spinach chloroplastic carbonic anhydrase nucleotide sequence analysis of cDNA. Plant Physiol 92(1):37–40

Calvin M, Bassham JA, Benson AA, Lynch V, Ouellet C, Schou L, Stepka Wt, Tolbert NE (1950) The path of carbon in photosynthesis. X. Carbon dioxide assimilation in plants. Lawrence Berkeley National Laboratory

Carrae-Mlouka A, Maejean A, Quillardet P, Ashida H, Saito Y, Yokota A, Callebaut I, Sekowska A, Dittmann E, Bouchier C (2006) A new RuBisCO-like protein coexists with a photosynthetic RuBisCO in the planktonic cyanobacteria *Microcystis*. J Biol Chem 281(34):24462–24471

Chollet R, Vidal J, O'Leary MH (1996) Phospho enol pyruvate carboxylase: a ubiquitous, highly regulated enzyme in plants. Annu Rev Plant Biol 47(1):273–298

Clegg MT, Cummings MP, Durbin ML (1997) The evolution of plant nuclear genes. Proc Natl Acad Sci 94(15):7791–7798

Cot SSW, So AKC, Espie GS (2008) A multiprotein bicarbonate dehydration complex essential to carboxysome function in cyanobacteria. J Bacteriol 190(3):936–945

Covarrubias AS, Bergfors T, Jones TA, Hogbom M (2006) Structural mechanics of the pH-dependent activity of beta-carbonic anhydrase from *Mycobacterium tuberculosis*. J Biol Chem 281(8):4993–4999

Daley SME, Kappell AD, Carrick MJ, Burnap RL (2012) Regulation of the cyanobacterial CO_2-concentrating mechanism involves internal sensing of $NADP^+$ and α-ketogutarate levels by transcription factor CcmR. PLoS ONE 7(7):e41286

Derelle E, Ferraz C, Rombauts S, Rouza P, Worden AZ, Robbens S, Partensky Fdr, Degroeve S, Echeynia S, Cooke R (2006) Genome analysis of the smallest free-living eukaryote Ostreococcus tauri unveils many unique features. Proc Nat Acad Sci 103(31):11647–11652

Donaldson TL, Quinn JA (1974) Kinetic constants determined from membrane transport measurements: carbonic anhydrase activity at high concentrations. Proc Natl Acad Sci 71(12):4995–4999

Ducat DC, Silver PA (2012) Improving carbon fixation pathways. Curr Opin Chem Biol 16(3):337–344

Dufossae L, Galaup P, Yaron A, Arad SM, Blanc P, Chidambara Murthy KN, Ravishankar GA (2005) Microorganisms and microalgae as sources of pigments for food use: a scientific oddity or an industrial reality? Trends Food Sci Technol 16(9):389–406

Ellis RJ (1979) The most abundant protein in the world. Trends Biochem Sci 4(11):241–244

Emlyn-Jones D, Woodger FJ, Price GD, Whitney SM (2006) RbcX can function as a RubBisCO chaperonin, but is non-essential in *Synechococcus* PCC7942. Plant Cell Physiol 47(12):1630–1640

Eriksson AE, Jones TA, Liljas A (1988) Refined structure of human carbonic anhydrase II at 2.0 Å resolution. Proteins Struct Funct Bioinf 4(4):274–282

Eriksson M, Karlsson J, Ramazanov Z, Gardestrom P, Samuelsson G (1996) Discovery of an algal mitochondrial carbonic anhydrase: molecular cloning and characterization of a low-CO_2-induced polypeptide in *Chlamydomonas reinhardtii*. Proc Natl Acad Sci 93(21):12031–12034

Falkowski PG, Raven JA (1997) Aquatic photosynthesis. Blackwell Science, New Jersey

Fawcett TW, Volokita M, Bartlett SG (1990) Spinach carbonic anhydrase primary structure deduced from the sequence of a cDNA clone. J Biol Chem 265(10):5414–5417

Ferguson JKW, Lewis L, Smith J (1937) The distribution of carbonic anhydrase in certain marine invertebrates. J Cell Comp Physiol 10(3):395–400

Flores-Paerez Ã, Jarvis P (2013) Molecular chaperone involvement in chloroplast protein import. Biochimica et Biophysica Acta (BBA)-Mol Cell Res 1833(2):332–340

Fukuzawa H, Fujiwara S, Yamamoto Y, Dionisio-Sese ML, Miyachi S (1990) cDNA cloning, sequence, and expression of carbonic anhydrase in *Chlamydomonas reinhardtii*: regulation by environmental CO_2 concentration. Proc Natl Acad Sci 87(11):4383–4387

Fukuzawa H, Suzuki E, Komukai Y, Miyachi S (1992) A gene homologous to chloroplast carbonic anhydrase (*icfA*) is essential to photosynthetic carbon dioxide fixation by *Synechococcus* PCC7942. Proc Natl Acad Sci 89(10):4437–4441

Furbank RT, Taylor WC (1995) Regulation of photosynthesis in C_3 and C_4 plants: a molecular approach. Plant Cell 7(7):797

Gilbert BC, Murphy DM, Chechik V (2012) Electron paramagnetic resonance. Royal Society of Chemistry, UK

Green B, Parson WW (2003) Light-harvesting antennas in photosynthesis. Springer, New York

Haimovichae Dayan M, Garfinkel N, Ewe D, Marcus Y, Gruber A, Wagner H, Kroth PG, Kaplan A (2013) The role of C_4 metabolism in the marine diatom *Phaeodactylum tricornutum*. New Phytol 197(1):177–185

Hanson TE, Tabita FR (2001) A ribulose-1, 5-bisphosphate carboxylase/oxygenase (RuBisCO)-like protein from *Chlorobium tepidum* that is involved with sulfur metabolism and the response to oxidative stress. Proc Natl Acad Sci 98(8):4397–4402

Hatch MD, Slack CR (1966) Photosynthesis by sugar-cane leaves. Biochem J 101:103–111

Heinhorst S, Williams EB, Cai F, Murin CD, Shively JM, Cannon GC (2006) Characterization of the carboxysomal carbonic anhydrase CsoSCA from *Halothiobacillus neapolitanus*. J Bacteriol 188(23):8087–8094

Hewett-Emmett D, Tashian RE (1996) Functional diversity, conservation, and convergence in the evolution of the α-, β-, and γ-carbonic anhydrase gene families. Mol Phylogenet Evol 5(1):50–77

Hiltonen T, Björkbacka H, Forsman C, Clarke AK, Samuelsson G (1998) Intracellular β-carbonic anhydrase of the unicellular green alga *Coccomyxa* cloning of the cDNA and characterization of the functional enzyme overexpressed in *Escherichia coli*. Plant Physiol 117(4):1341–1349

Huang S, Hainzl T, Grundstrom C, Forsman C, Samuelsson G, Sauer-Eriksson AE (2011) Structural studies of β-carbonic anhydrase from the green alga *Coccomyxa*: inhibitor complexes with anions and acetazolamide. PLoS ONE 6(12):e28458

Iverson TM, Alber BE, Kisker C, Ferry JG, Rees DC (2000) A closer look at the active site of γ-class carbonic anhydrases: high-resolution crystallographic studies of the carbonic anhydrase from *Methanosarcina thermophila*. Biochemistry 39(31):9222–9231

Kanth BK, Min K, Kumari S, Jeon H, Jin ES, Lee J, Pack SP (2012) Expression and characterization of codon-optimized carbonic anhydrase from *Dunaliella* species for CO_2 sequestration application. Appl Biochem Biotechnol 167(8):2341–2356

Karkehabadi S (2005) Structure-function studies of ribulose-1, 5-bisphosphate carboxylase/oxygenase: activation, thermostability, and CO_2/O_2 specificity, vol 2005

Keeley JE (1998) C_4 photosynthetic modifications in the evolutionary transition from land to water in aquatic grasses. Oecologia 116(1–2):85–97

Keeley JE, Sternberg LO, Deniro MJ (1986) The use of stable isotopes in the study of photosynthesis in freshwater plants. Aquat Bot 26:213–223

Kennedy RA (1976) Photorespiration in C_3 and C_4 plant tissue cultures significance of Kranz Anatomy to low photorespiration in C_4 Plants. Plant Physiol 58(4):573–575

Kimber MS, Pai EF (2000) The active site architecture of *Pisum sativum* β-carbonic anhydrase is a mirror image of that of α-carbonic anhydrases. EMBO J 19(7):1407–1418

Kirk JTO (1994) Light and photosynthesis in aquatic ecosystems. Cambridge University Press, Cambridge

Kisker C, Schindelin H, Alber BE, Ferry JG, Rees DC (1996) A left-hand beta-helix revealed by the crystal structure of a carbonic anhydrase from the archaeon *Methanosarcina thermophila*. The EMBO J 15(10):2323

Kremer BP, Kuppers U (1977) Carboxylating enzymes and pathway of photosynthetic carbon assimilation in different marine algae-Evidence for the C_4-pathway? Planta 133(2):191–196

Krishnamurthy VM, Kaufman GK, Urbach AR, Gitlin I, Gudiksen KL, Weibel DB, Whitesides GM (2008) Carbonic anhydrase as a model for biophysical and physical-organic studies of proteins and protein-ligand binding. Chem Rev 108(3):946–1051

Krissinel E, Henrick K (2007) Inference of macromolecular assemblies from crystalline state. J Mol Biol 372(3):774–797

Kröncke K-D, Klotz L-O (2009) Zinc fingers as biologic redox switches? Antioxid Redox Signal 11(5):1015–1027

Kumar S, Singh V, Tiwari M (2007) Quantitative structure activity relationship studies of sulfamide derivatives as carbonic anhydrase inhibitor: as antiglaucoma agents. Med Chem 3(4):379–386

Laing WA, Ogren WL, Hageman RH (1974) Regulation of soybean net photosynthetic CO_2 fixation by the interaction of CO_2, O_2, and ribulose 1, 5-diphosphate carboxylase. Plant Physiol 54(5):678–685

Lapointe M, MacKenzie TDB, Morse D (2008) An external delta-carbonic anhydrase in a free-living marine dinoflagellate may circumvent diffusion-limited carbon acquisition. Plant Physiol 147(3):1427–1436

Larimer FW, Soper TS (1993) Overproduction of *Anabaena* 7120 ribulose-bisphosphate carboxylase/oxygenase in *Escherichia coli*. Gene 126(1):85–92

Liljas A, Kannan KK, Bergsten PC, Waara I, Fridborg K, Strandberg B, Carlbom U, Järup L, Lagren S, Petef M (1972) Crystal structure of human carbonic anhydrase C. Nature 235(57):131–137

Liu C, Young AL, Starling-Windhof A, Bracher A, Saschenbrecker S, Rao BV, Rao KV, Berninghausen O, Mielke T, Hartl FU (2010) Coupled chaperone action in folding and assembly of hexadecameric RuBisco. Nature 463(7278):197–202

McGrath JM, Long SP (2014) Can the cyanobacterial carbon-concentrating mechanism increase photosynthesis in crop species? A theoretical analysis. Plant Physiol 164(4):2247–2261

Mitsuhashi S, Mizushima T, Yamashita E, Yamamoto M, Kumasaka T, Moriyama H, Ueki T, Miyachi S, Tsukihara T (2000) X-ray structure of beta-carbonic anhydrase from the red alga, *Porphyridium purpureum*, reveals a novel catalytic site for CO_2 hydration. J Biol Chem 275(8):5521–5526

Morita K, Hatanaka T, Misoo S, Fukayama H (2014) Unusual small subunit that is not expressed in photosynthetic cells alters the catalytic properties of RuBisco in rice. Plant Physiol 164(1):69–79

Moroney JV, Ma Y, Frey WD, Fusilier KA, Pham TT, Simms TA, DiMario RJ, Yang J, Mukherjee B (2011) The carbonic anhydrase isoforms of *Chlamydomonas reinhardtii*: intracellular location, expression, and physiological roles. Photosynth Res 109(1–3):133–149

Moroney JV, Ynalvez RA (2007) Proposed carbon dioxide concentrating mechanism in *Chlamydomonas reinhardtii*. Eukaryot Cell 6(8):1251–1259

Mukherjee B (2013) Investigation of the role of putative inorganic carbon transporters in the carbon dioxide concentrating mechanisms of *Chlamydomonas reinhardtii*. Calcutta University, Kolkata

Newman J, Gutteridge S (1993) The X-ray structure of *Synechococcus* ribulose-bisphosphate carboxylase/oxygenase-activated quaternary complex at 2.2-A resolution. J Biol Chem 268(34):25876–25886

Nishitani Y, Yoshida S, Fujihashi M, Kitagawa K, Doi T, Atomi H, Imanaka T, Miki K (2010) Structure-based catalytic optimization of a type III RuBisco from a hyperthermophile. J Biol Chem 285(50):39339–39347

Ogren WL (1984) Photorespiration: pathways, regulation, and modification. Annu Rev Plant Physiol 35(1):415–442

Onizuka T, Endo S, Akiyama H, Kanai S, Hirano M, Yokota A, Tanaka S, Miyasaka H (2004) The *rbcX* gene product promotes the production and assembly of ribulose-1, 5-bisphosphate carboxylase/oxygenase of *Synechococcus* sp. PCC7002 in *Escherichia coli*. Plant Cell Physiol 45(10):1390–1395

Parkin G (2004) Synthetic analogues relevant to the structure and function of zinc enzymes. Chem Rev 104(2):699–768

Pastorek J, Pastorekova S, Callebaut I, Mornon JP, Zelník V, Opavska R, Zat'ovicová M, Liao S, Portetelle D, Stanbridge EJ (1994) Cloning and characterization of MN, a human tumor-associated protein with a domain homologous to carbonic anhydrase and a putative helix-loop-helix DNA binding segment. Oncogene 9(10):2877–2888

Peña KL, Castel SE, de Araujo C, Espie GS, Kimber MS (2010) Structural basis of the oxidative activation of the carboxysomal gamma-carbonic anhydrase, CcmM. Proc Natl Acad Sci 107(6):2455–2460

Portis AR Jr (1992) Regulation of ribulose 1, 5-bisphosphate carboxylase/oxygenase activity. Annu Rev Plant Biol 43(1):415–437

Portis AR Jr (2003) RuBisco activase "RuBisco's catalytic chaperone". Photosynth Res 75(1):11–27

Portis AR Jr, Parry MAJ (2007) Discoveries in RuBisco (Ribulose 1, 5-bisphosphate carboxylase/oxygenase): a historical perspective. Photosynth Res 94(1):121–143

Price GD (2011) Inorganic carbon transporters of the cyanobacterial CO_2 concentrating mechanism. Photosynth Res 109(1–3):47–57

Price GD, Badger MR, Woodger FJ, Long BM (2008) Advances in understanding the cyanobacterial CO_2-concentrating-mechanism (CCM): functional components, C_i transporters, diversity, genetic regulation and prospects for engineering into plants. J Exp Bot 59(7):1441–1461

Rae BD, Long BM, Badger MR, Price GD (2013) Functions, compositions, and evolution of the two types of carboxysomes: polyhedral microcompartments that facilitate CO_2 fixation in cyanobacteria and some proteobacteria. Microbiol Mol Biol Rev 77(3):357–379

Raines CA (2011) Increasing photosynthetic carbon assimilation in C_3 plants to improve crop yield: current and future strategies. Plant Physiol 155(1):36–42

Rao SK, Fukayama H, Reiskind JB, Miyao M, Bowes G (2006) Identification of C_4 responsive genes in the facultative C_4 plant *Hydrilla verticillata*. Photosynth Res 88(2):173–183

Raven JA (1997) CO_2-concentrating mechanisms: a direct role for thylakoid lumen acidification? Plant Cell Environ 20(2):147–154

Raven JA, Cockell CS, De La Rocha CL (2008) The evolution of inorganic carbon concentrating mechanisms in photosynthesis. Philos Trans R Soc B Biol Sci 363(1504):2641–2650

Reinfelder JR (2011) Carbon concentrating mechanisms in eukaryotic marine phytoplankton. Ann Rev Mar Sci 3:291–315

Reiskind JB, Bowes G (1991) The role of phosphoenolpyruvate carboxykinase in a marine macroalga with C_4-like photosynthetic characteristics. Proc Natl Acad Sci 88(7):2883–2887

Reiskind JB, Seamon PT, Bowes G (1988) Alternative methods of photosynthetic carbon assimilation in marine macroalgae. Plant Physiol 87(3):686–692

Roberts SB, Lane TW, Morel FoMM (1997) Carbonic anhydrase in the marine diatom *Thalassiosira weissflogii* (Bacillariophyceae) 1. J Phycol 33(5):845–850

Rudi K, Skulberg OM, Jakobsen KS (1998) Evolution of cyanobacteria by exchange of genetic material among phyletically related strains. J Bacteriol 180(13):3453–3461

Sage RF (2002) Variation in the k_{cat} of RuBisco in C_3 and C_4 plants and some implications for photosynthetic performance at high and low temperature. J Exp Bot 53(369):609–620

Saschenbrecker S (2007) Folding and assembly of RuBisCO. Ph.D. thesis, lmu

Saschenbrecker S, Bracher A, Rao KV, Rao BV, Hartl FU, Hayer-Hartl M (2007) Structure and function of RbcX, an assembly chaperone for hexadecameric RuBisco. Cell 129(6):1189–1200

Sawaya MR, Cannon GC, Heinhorst S, Tanaka S, Williams EB, Yeates TO, Kerfeld CA (2006) The structure of β-carbonic anhydrase from the carboxysomal shell reveals a distinct subclass with one active site for the price of two. J Biol Chem 281(11):7546–7555

Schlicker C, Hall RA, Vullo D, Middelhaufe S, Gertz M, Supuran CT, Mahlschlegel FA, Steegborn C (2009) Structure and inhibition of the CO_2-sensing carbonic anhydrase Can2 from the pathogenic fungus *Cryptococcus neoformans*. J Mol Biol 385(4):1207–1220

Schneider G, Lindqvist Y, Lundqvist T (1990) Crystallographic refinement and structure of ribulose-1, 5-bisphosphate carboxylase from *Rhodospirillum rubrum* at 1.7 Å resolution. J Mol Biol 211(4):989–1008

Scholes GD, Fleming GR (2005) Energy transfer and photosynthetic light harvesting. Adv Chem Phys 132:57–130

Schuster G, Owens GC, Cohen Y, Ohad I (1984) Thylakoid polypeptide composition and light-independent phosphorylation of the chlorophyll *a, b*-protein in *Prochloron*, a prokaryote exhibiting oxygenic photosynthesis. Biochimica et Biophysica Acta (BBA)-Bioenerg 767(3):596–605

Shiba T, Simidu U, Taga N (1979) Distribution of aerobic bacteria which contain bacteriochlorophyll a. Appl Environ Microbiol 38(1):43–45

Smith KS, Ferry JG (1999) A plant-type (β-class) carbonic anhydrase in the thermophilic methanoarchaeon *Methanobacterium thermoautotrophicum*. J Bacteriol 181(20):6247–6253

Smith MR, Mah RA (1978) Growth and methanogenesis by *Methanosarcina* strain 227 on acetate and methanol. Appl Environ Microbiol 36(6):870–879

So AKC, Espie GS (2005) Cyanobacterial carbonic anhydrases. Can J Bot 83(7):721–734

So AKC, Espie GS, Williams EB, Shively JM, Heinhorst S, Cannon GC (2004) A novel evolutionary lineage of carbonic anhydrase (ε-class) is a component of the carboxysome shell. J Bacteriol 186(3):623–630

Soltes-Rak E, Mulligan ME, Coleman JR (1997) Identification and characterization of a gene encoding a vertebrate-type carbonic anhydrase in cyanobacteria. J Bacteriol 179(3):769–774

Spreitzer RJ, Salvucci ME (2002) RuBisCO: structure, regulatory interactions, and possibilities for a better enzyme. Annu Rev Plant Biol 53(1):449–475

Sugawara H, Yamamoto H, Shibata N, Inoue T, Okada S, Miyake C, Yokota A, Kai Y (1999) Crystal structure of carboxylase reaction-oriented ribulose 1, 5-bisphosphate carboxylase/oxygenase from a thermophilic red alga, *Galdieria partita*. J Biol Chem 274(22):15655–15661

Sugiyama T, Mizuno M, Hayashi M (1984) Partitioning of nitrogen among ribulose-1, 5-bisphosphate carboxylase/oxygenase, phosphoenolpyruvate carboxylase, and pyruvate orthophosphate dikinase as related to biomass productivity in maize seedlings. Plant Physiol 75(3):665–669

Supuran CT (2011) Carbonic anhydrase inhibition with natural products: novel chemotypes and inhibition mechanisms. Mol Divers 15(2):305–16. doi:101007/s11030-010-9271-4 (Epub 2010 Aug 28)

Supuran CT, Scozzafava A (2007) Carbonic anhydrases as targets for medicinal chemistry. Bioorg Med Chem 15(13):4336–4350

Tabita FR (1999) Microbial ribulose 1, 5-bisphosphate carboxylase/oxygenase: a different perspective. Photosynth Res 60(1):1–28

Tabita FR, Hanson TE, Li H, Satagopan S, Singh J, Chan S (2007) Function, structure, and evolution of the RuBisCO-like proteins and their RuBisCO homologs. Microbiol Mol Biol Rev 71(4):576–599

Tabita FR, Satagopan S, Hanson TE, Kreel NE, Scott SS (2008) Distinct form I, II, III, and IV RuBisCO proteins from the three kingdoms of life provide clues about RuBisCO evolution and structure/function relationships. J Exp Bot 59(7):1515–1524

Taylor TC, Andersson I (1997) The structure of the complex between RuBisCO and its natural substrate ribulose 1, 5-bisphosphate. J Mol Biol 265(4):432–444

Tetu SG, Tanz SK, Vella N, Burnell JN, Ludwig M (2007) The Flaveria bidentis β-carbonic anhydrase gene family encodes cytosolic and chloroplastic isoforms demonstrating distinct organ-specific expression patterns. Plant Physiol 144(3):1316–1327

Tripp BC, Smith K, Ferry JG (2001) Carbonic anhydrase: new insights for an ancient enzyme. J Biol Chem 276(52):48615–48618

Tsuzuki M, Miyachi S (1989) The function of carbonic anhydrase in aquatic photosynthesis. Aquat Bot 34(1):85–104

Van Gorkom HJ (1985) Electron transfer in photosystem II. Photosynth Res 6(2):97–112

van Lun M, Hub JS, van der Spoel D, Andersson I (2014) CO_2 and O_2 distribution in RuBisco Suggests the small subunit functions as a CO_2 reservoir. J Am Chem Soc 136(8):3165–3171

van Ooijen G, Knox K, Kis K, Bouget F-Y, Millar AJ (2012) Genomic transformation of the picoeukaryote *Ostreococcus tauri*. J Vis Exp JoVE (65)

Vega MC, Lorentzen E, Linden A, Wilmanns M (2003) Evolutionary markers in the (β/α)8-barrel fold. Curr Opin Chem Biol 7(6):694–701

Walker JCG (1985) Carbon dioxide on the early Earth. Orig Life Evol Biosph 16(2):117–127

Wang Q, Fristedt R, Yu X, Chen Z, Liu H, Lee Y, Guo H, Merchant SS, Lin C (2012) The γ-carbonic anhydrase subcomplex of mitochondrial complex I is essential for development and important for photomorphogenesis of *Arabidopsis*. Plant Physiol 160(3):1373–1383

Wang X, Wu S, Xu D, Xie D, Guo H (2011) Inhibitor and substrate binding by angiotensin-converting enzyme: quantum mechanical/molecular mechanical molecular dynamics studies. J Chem Inf Model 23; 51(5):1074–1082. doi:101021/ci200083f (Epub 2011 Apr 26)

Warlick B (2013) Functional discovery and promiscuity in the RuBisCO superfamily. University of Illinois at Urbana-Champaign, USA

Whitmarsh J (1999) The photosynthetic process. In: Concepts in photobiology. Springer, pp 11–51

Whitney SM, Andrews TJ (2001) The gene for the ribulose-1, 5-bisphosphate carboxylase/oxygenase (RuBisco) small subunit relocated to the plastid genome of tobacco directs the synthesis of small subunits that assemble into RuBisCO. Plant Cell Online 13(1):193–205

Whitney SM, Houtz RL, Alonso H (2011) Advancing our understanding and capacity to engineer nature's CO_2-sequestering enzyme, RuBisCO. Plant physiol 155(1):27–35

Windhof A (2011) RuBisco folding and oligomeric assembly: detailed analysis of an assembly intermediate. lmu

Xu J, Fan X, Zhang X, Xu D, Mou S, Cao S, Zheng Z, Miao J, Ye N (2012) Evidence of coexistence of C_3 and C_4 photosynthetic pathways in a green-tide-forming alga, *Ulva prolifera*. PloS one 7(5):e37438

Yurkov V, Beatty JT (1998) Isolation of aerobic anoxygenic photosynthetic bacteria from black smoker plume waters of the juan de fuca ridge in the pacific ocean. Appl Environ Microbiol 64(1):337–341

Zastrow ML, Pecoraro VL (2013) Influence of active site location on catalytic activity in de novo-designed zinc metalloenzymes. J Am Chem Soc 135(15):5895–5903

http://www.springer.com/978-3-319-09122-8

Photosynthetic Microorganisms
Mechanism For Carbon Concentration
Singh, S.K.; Sundaram, S.; Kishor, K.
2014, X, 123 p. 27 illus., 26 illus. in color., Softcover
ISBN: 978-3-319-09122-8